# EDGE EFFECTS OF SHORELINE ARMORING -

# AN ASSESSMENT OF UNMANNED AERIAL SYSTEMS AS A TOOL FOR MONITORING SALT MARSH EROSION

**by**

**COURTNEY BALLING**

**(Under the Direction of Mark Risse)**

## ABSTRACT

Coastal properties at risk of erosion have traditionally been protected by hard armoring structures, e.g. bulkheads or seawalls. Hardened shorelines reduce essential intertidal habitat and have been shown to interrupt sediment dynamics at multiple spatial scales, often increasing erosion on adjacent properties. The “living shoreline” utilizes native plant materials and reef structures to hold sediments in place, thus providing ecosystem services while protecting upland properties. Despite numerous studies of the ecological benefits of living shorelines, their effects on adjacent properties are not well known. Over the course of one hurricane season, the banks adjacent to three living shorelines and three bulkheads were evaluated using an unmanned aerial system and erosion rates calculated using Structure-from-Motion. Statistically significant differences in erosion were not observed between the two groups, however scouring was evident immediately adjacent to each bulkhead site and living shoreline sites appeared less variable over time.

**INDEX WORDS:** Living shoreline, Bulkhead, Shoreline Armoring, Coastal erosion, Unmanned aerial system, Structure-from-Motion, Salt marsh

# EDGE EFFECTS OF SHORELINE ARMORING -

# AN ASSESSMENT OF UNMANNED AERIAL SYSTEMS AS A TOOL FOR MONITORING SALT MARSH EROSION

**by**

**COURTNEY BALLING**

**B.S., The University of Vermont, 2015**

**A Thesis Submitted to the Graduate Faculty of The University of Georgia in Partial Fulfillment**

**of the Requirements for the Degree**

**MASTER OF SCIENCE**

**ATHENS, GEORGIA**

**2018**

**© 2018**

**Courtney Balling**

**All Rights Reserved**

# EDGE EFFECTS OF SHORELINE ARMORING -

# AN ASSESSMENT OF UNMANNED AERIAL SYSTEMS AS A TOOL FOR MONITORING SALT MARSH EROSION

**by**

**COURTNEY BALLING**

**Major Professor: Mark Risse**

**Committee: Clark Alexander**

**Thomas Bliss**

**Electronic Version Approved:**

**Suzanne Barbour**

**Dean of the Graduate School**

**The University of Georgia**

**August 2018**

## DEDICATION

**For my eternally loving husband, Sam, always game for an adventure.**

## ACKNOWLEDGEMENTS

**I would like to acknowledge my Major Professor, Mark Risse, for the opportunity to join a wonderful scientific community and for his guidance and patience throughout this process. I would also like to thank my committee members, Clark Alexander and Thomas Bliss for their support, advice, and expertise. This research would not have been possible without the technical expertise and field assistance of Tommy Jordan and Marguerite Madden. Many thanks as well to the land owners who so graciously allowed us access to their property, including the St. Simons Land Trust, Little St. Simons Island, The Burton 4H Center, and many private homeowners. Finally, I would like to thank my family and friends for their endless love and support.**

## TABLE OF CONTENTS

**Page**

## LIST OF TABLES

**Page**

## LIST OF FIGURES

**Page**

# CHAPTER 1

# INTRODUCTION

Global climate change, sea level rise, and increased storm intensity necessitate research into new methods of erosion control to protect coastal communities, ecology, and natural resources (Gittman, Popowich, Bruno, & Peterson, 2014). Traditionally, coastal erosion control has been accomplished using hard armoring structures (e.g. bulkheads, seawalls, rip rap, or revetments). This "hardening" of our coastlines comes with costs, however, as traditional built infrastructure can interrupt coastal sediment dynamics, exacerbate erosion on adjacent properties, and remove the natural ability of coastal ecosystems to respond to sea level rise. As coastal populations and development increases, understanding the effects of these structures at multiple spatial scales is essential to managing coastal resources sustainably.

An emerging technique in erosion control is that of the "living shoreline", a man-made structure comprised of natural, living materials that is designed to hold upland soil in place in the same manner as bulkheads, rip rap, etc. The ecological benefits of living shorelines have been widely documented, but long-term data concerning their physical effectiveness and impact is still needed. *Spartina alterniflora*, the primary plant species used in living shorelines on the Southeast Atlantic coast, has a great capacity to affect the flow of water and sediments, perhaps in quite a different manner than hard armoring (Bilkovic, Mitchell, Mason, & Duhring, 2016). However, few direct comparisons have

been made of the edge effects of hardened shorelines versus living shorelines, particularly in the high tidal range experienced on the Georgia coast.

One challenge to quantifying the effects of shoreline armoring is the lack of affordable, accessible methods of reconstructing topography at a high spatial resolution to assess volumetric changes in sediment over time. This research aimed to quantify the differences in edge effects of bulkheads and living shorelines using a method of three-dimensional topographic reconstruction – Structure from Motion (SfM). SfM utilizes imagery, commonly acquired from unmanned aerial systems (UAS), to recreate three-dimensional structure. Its affordability and ease of use make it a promising tool for the collection of high-resolution three-dimensional data over large spatial extents and at high temporal resolutions.

Over the course of one year, UAS imagery and ground measurements were acquired from areas both fifty meters upstream and downstream from three bulkheads and three living shorelines in tidally influenced rivers on the Georgia Coast. Three major data collection events—at the onset of hurricane season, immediately following hurricane Irma, and four months following the storm—allowed for an analysis of the effects of each armoring type on adjacent properties under both routine and extreme conditions. The use of UAS imagery as a data collection tool also allowed for an analysis of the effectiveness of the SfM method in monitoring salt marsh change.

### *Consequences of Shoreline Armoring*

Coastal development is increasing at a rapid pace, with over one-third of the world's population living within 100 kilometers of a coast line (Gittman et al., 2015; MA, 2005).

This number is even greater in the continental United States, where coastal counties occupy only 17% of the land area but are home to 53% of the population (Manis, Garvis, Jachec, & Walters, 2015). Many of these coastal properties are eroding due to wave action, storm events, flooding, and sea level rise, necessitating the installation of shoreline armoring structures. These structures, such as sea walls, bulkheads, or rip rap, commonly consist of vertical concrete or wooden walls or sloped rock structures placed directly on a shoreline to hold upland soil in place (Gittman, Peterson, et al., 2016; O'Donnell, 2017; Scyphers, Powers, Heck, & Byron, 2011; Theuerkauf, Eggleston, Puckett, & Theuerkauf, 2017). This "shoreline hardening" has been the most common response to coastal erosion but can have negative ecological as well as physical impacts. Hardened shorelines have been found to increase erosion rates at multiple spatial scales due to wave reflection and interference with sediment transport (Nordstrom, Jackson, Rafferty, Raineault, & Grafals-Soto, 2009; NRC, 2007; Wakefield, 2016), and are associated with adverse effects on adjacent properties, increased scouring and turbidity, and a shorter and steeper intertidal zone. Hardened structures also contribute to habitat loss and fragmentation, loss of species diversity, and increases in invasive species (Balouskus & Targett, 2016; Bilkovic et al., 2016; Bilkovic & Mitchell, 2013; Bilkovic & Roggero, 2008; Gittman et al., 2015; Manis et al., 2015; O'Donnell, 2017; Scyphers, Picou, & Powers, 2015; Scyphers, Powers, & Heck, 2015; Scyphers et al., 2011; Theuerkauf et al., 2017). An estimated 14% of the U.S. shoreline was hardened as of 2015, leading to widespread loss of ecosystem services. (Gittman et al., 2015). Furthermore, these structures are unable to adapt to changing sea-levels or coastal conditions, thus becoming less effective over time and requiring regular repair or

replacement (O'Donnell, 2017). Hardened structures interrupt the natural land-sea ecotone that is essential to many species (Toft, Ogston, Heerhartz, Cordell, & Flemer, 2013) and may also increase scour during storm events and prevent coastal wetlands from keeping pace with sea level rise (Bilkovic et al., 2016; Gittman et al., 2015). The combined effects of armoring and sea level rise on the intertidal zone are referred to as "coastal squeeze", and result in net losses of intertidal land area (Toft et al., 2013). The myriad resources that our coastal communities have to offer—be they ecological, economic, or cultural—stand to suffer if new and innovative technologies are not explored.

If hardening continues at the current rate, approximately one third of the US coastline will be armored by the year 2100 (Gittman et al., 2015). Hardening is most common in areas that experience frequent storm events, however dunes and natural marsh lands have been shown to suffer less damage during storms than bulkheads or seawalls. This supports an argument for keeping natural shorelines intact and using natural infrastructure in place of hard materials whenever possible (Gittman et al., 2015; Gittman et al., 2014). Possibly counterintuitively, hardening is also more common in sheltered coastal areas than in open areas, with 64% of hardening occurring in marshes, lagoons, and tidal creeks (Gittman, Scyphers, Smith, Neylan, & Grabowski, 2016). Estuarine habitats comprise only 0.7% of global ecosystems yet are estimated to contribute 23.7% of ecosystem services (Scyphers et al., 2011). The current trend of armoring these sensitive and valuable estuarine shorelines does not provide an optimistic outlook for their future. Fifty percent of U.S. salt marshes have been lost over the past one hundred years, largely due to human activity and development (Kennish, 2001). Increased

development in the Southeast Atlantic and Gulf coasts alone threatens over half of the remaining salt marsh and all U.S. mangrove forests (Gittman et al., 2015). Research suggests that landowners partially base their decision to install hard armoring on the increased erosion or wave energy that results from neighboring armoring structures, indicating that the decision of one landowner can create a domino effect along coastlines. This pattern has been observed in many coastal communities, as development and armoring in one area may interrupt sediment dynamics and exacerbate erosion in another. Thus, one armoring structure begets another, and another, until large portions of intertidal land are effectively eliminated (Scyphers, Picou, et al., 2015).

### *Living Shorelines – A New Alternative*

An alternative erosion control technique to such structures is the "living shoreline". The National Oceanic and Atmospheric Association (NOAA) defines living shorelines as a "shoreline management practice that provides erosion control benefits; protects, restores or enhances natural shoreline habitat; and maintains coastal processes through the strategic placement of plants, stone, sand fill, and other structural organic materials (e.g., biologs, oyster reefs, etc.)", though definitions also vary by state (O'Donnell, 2017). This approach relies heavily on native wetland species to attenuate wave and flood erosion, stabilize sediments, reduce surface runoff, and keep pace with sea level rise, all while providing a host of other ecosystem services (O'Donnell, 2017; Theuerkauf et al., 2017). Living shorelines can be less expensive to install than hard armoring structures and require less maintenance once established, as, with proper site selection and design, these natural structures can be largely self-sustaining (Manis et al., 2015; O'Donnell, 2017). Not surprisingly, this type of "ecological engineering" can also

improve human connections to and appreciation for the environment (Toft et al., 2013). Each living shoreline project must be tailored specifically to the site in need, and thus fosters an intimate connection with and understanding of the landscape. Further, these structures do not simply remain static once installed. Comprised of living, growing organisms, these structures operate in a state of dynamic equilibrium, offering landowners an opportunity to act as stewards of their land and observe its self-healing properties first hand.

The design of living shorelines differs largely based on the specific coastal setting but may include natural or "soft" infrastructure alone, or a combination of both soft and hard materials, such as marsh plantings that are protected by a rip rap or oyster sill. Areas of low wave energy can benefit from living shorelines comprised entirely of soft infrastructure, but in areas exposed to large fetches or boat wakes, the addition of a sill or some other "hybrid" approach may be necessary to protect vegetation from wave energy (Balouskus & Targett, 2016; Manis et al., 2015; O'Donnell, 2017). These hard elements, however, should simply serve as support for vegetation, with the focus remaining on native species (Bilkovic et al., 2016). One study has shown that a hybrid living shoreline approach can actually be more effective at reducing boat wake energy than hard armoring alone and should be considered more often for high traffic areas (De Roo & Troch, 2015).

On the South Atlantic coast of the United states, two native species are commonly used in the construction of living shorelines - the eastern oyster (*Crassostrea virginica*) and smooth cordgrass (*Spartina alterniflora*). The native range of both *C. virginica* and *S. alterniflora* stretches from Canada to Mexico along the Atlantic and Gulf coasts, and

each have growth habits that make them ideal candidates for erosion control. *C. virginica* forms extensive subtidal and intertidal reefs, quickly increasing in area and elevation through the recruitment of free-swimming larvae onto existing oyster shell or another hard substrate (Colden, Fall, Cartwright, & Friedrichs, 2016; Manis et al., 2015). *S. alterniflora* thrives in the mid to upper intertidal zone, spreading through extensive rhizomes. The perennial grass reaches heights of 0.3-3 m and is capable of stem densities of up to 890 stems/$m^2$ (Manis et al., 2015; Sharma, Goff, Cebrian, & Ferraro, 2016). The species is extremely adaptable to transplant, with even hybrid living shorelines that incorporate rip rap sills having been shown to achieve species diversity and densities comparable to native stands of *S. alterniflora* (Balouskus & Targett, 2016). Each species, if grown under ideal conditions, can increase in elevation at such a rate as to outpace sea level rise (assuming, of course, that there is sufficient undeveloped upland land area for the marsh species to migrate *to*) (Rodriguez et al., 2014; Theuerkauf et al., 2017; Wang, Wang, & Chen, 2008). It should be noted that much of the previous research has been performed in low tidal ranges, and data collected from higher tidal ranges such as that of the Georgia coast is still needed.

Smooth cordgrass has long served as a natural defense against erosion along the Atlantic and Gulf coasts, making it an obvious choice for use in nature-based infrastructure. Stem height, stem density, and root density influence flow velocity, sediment distribution, and tidal creek pattern, as well as attenuate wave action (Bilkovic et al., 2016; O'Donnell, 2017; Wang et al., 2008). Flow velocity is rapidly slowed as water flows through a marsh, and studies have shown that the stems of *S. alterniflora* can attenuate wave height as much as 71% and wave velocity as much as 92% (Wang et al.,

2008). Flow velocities in the Chesapeake Bay have been observed to be 2-2.5 times greater in areas of open water than in vegetated areas (Leonard, Wren, & Beavers, 2002). This slowing of current velocity results in higher rates of sedimentation than are found on un-vegetated mudflats. Sediments are then held firmly in place by extensive networks of rhizomes and roots that may extend more than a meter into the ground. This sedimentation process is essential to keeping pace with sea level rise, as marshes can gain elevation with each tide as fresh sediment is deposited. The presence of native vegetation can not only mitigate erosion, but even lead to shoreline accretion under optimal conditions (Manis et al., 2015; Wang et al., 2008). Stem densities and sediment trapping capacities similar to that of natural marshes have been observed in restored marsh plantings within 2-3 years, and marsh-sill hybrid approaches have enabled stem densities higher than natural marshes within 5-10 years (Bilkovic & Mitchell, 2013; Sharma et al., 2016). Salt marshes in areas of high tidal range and high suspended sediment concentrations, such as the Georgia coast, are expected to perform especially well at keeping pace with sea level rise (O'Donnell, 2017). These erosion control benefits are evident not only in large expanses of marsh grass, but also along the marsh edge and in smaller, narrower stands of *Spartina*. Narrow strips of marsh vegetation are extremely effective at trapping sediment and filtering nutrients, particularly nitrate (Bilkovic et al., 2016; Bilkovic & Mitchell, 2013), and studies have shown that sedimentation is actually greater on the marsh edge (in the first 10 m) than in the marsh center (Bilkovic & Mitchell, 2013; Leonard et al., 2002). Living shorelines typically mimic this narrow edge habitat and can attain similar vegetation characteristics (stem height and density) within a short number of growing seasons (Bilkovic et al., 2016). With this data in mind, it can be

hypothesized that in areas where armoring is necessary, living shorelines may offer a much stronger defense against the effects of sea level rise than hard armoring structures, which stop the upland migration of marsh species all together.

The eastern oyster, the second species most commonly used in living shoreline construction, reduces erosion rates through physically stabilizing sediments beneath their extensive three-dimensional reefs, and increasing sedimentation by reducing flow rates and attenuating wave erosion (Colden et al., 2016; Rodriguez et al., 2014; Theuerkauf et al., 2017). Oyster reefs and breakwaters have been shown to reduce shoreline loss and erosion by up to 40%. In a wave tank experiment, one-year old living shorelines comprised of *S. alterniflora* and *C. virginica* reduced wave energy by 67.3%. This was largely attributed to the increase in oyster reef height during that time, but also to the increase in cordgrass stem density. The wave attenuation effects of oyster reefs may be lessened during periods of high water, highlighting the need for further study in areas with a high tidal range (Manis et al., 2015). It should be noted, however, that even a lessened effect during periods of high water can be quite impactful, particularly during storm surge and flood events. In a study following the landfall of Hurricane Sandy in 2012, sediment cores taken from upland areas surrounding the New York Harbor showed an increase in flood overwash events correlated to European settlement and the destruction of native oyster reefs (Brandon, Woodruff, Orton, & Donnelly, 2016). The widespread loss of oyster reefs in the area due to overharvest, development, and declines in water quality have resulted in a 30-200% increase in storm event wave energy compared to the pre-European settlement era.

In addition to the erosion control capacity of oyster reefs, *C. virginica* provides invaluable ecosystem services including water filtration, essential estuarine habitat, and increased fisheries production (Colden et al., 2016; Humphries & La Peyre, 2015; Rodriguez et al., 2014). Astoundingly, a single oyster can filter up to 189 liters (50 gallons) of water per day (Couranz, 2018), and thus, the additive effect of a thriving oyster population on water quality should not be underestimated. Despite the importance of the species, greater than 85% of oyster reefs have been lost worldwide (Beck et al., 2011).

Beyond the physical and ecological data that supports the use of oysters and smooth cordgrass in protecting our coast, there is also an undeniable link between the peoples of the Southeast Atlantic and these two species. Each have a rich history here both economically and culturally. The influence of the oyster is all too evident—from midden piles and fortress ruins to modern tabby houses and gouged kayaks that have lingered too long at low tide. The oyster has sustained countless generations of families on the eastern seaboard, and Georgia led the nation in oyster production just a century ago (MAREX, 2018). Similarly, a mere mention of the Georgia coast immediately conjures images of endless marsh meadows—vast expanses of *Spartina alterniflora* forming an ocean of a different kind. It is impossible to imagine a thriving Atlantic coastline in the absence of these two ecosystem engineers, which provides all the more reason to promote their use in place of rock of wood whenever possible. Moving forward, it must be recognized that equally as important as quantitative data in promoting the use of living shorelines is a sense of place, a sense of home.

The multitude of benefits provided by living shorelines have been recognized by both state and federal agencies alike. Maryland and Connecticut have enacted legislative requirements for living shorelines to be installed in place of hard armoring where applicable, and North Carolina, Mississippi and Virginia offer expedited permits for living shorelines as incentive. Maryland, Virginia, and Texas also offer low interest loans for living shoreline installation, and Oregon and Virginia offer tax incentives to property owners with living shorelines installed. At a federal level NOAA, the Environmental Protection Agency (EPA), and the U.S. Army Corps of Engineers (USACE) have all expressed their support for living shorelines. NOAA and the USACE have also collaborated to form the Systems Approach to Geomorphic Engineering (SAGE), which serves as a community of practice focused on coastal protection and includes living shorelines as a conservation tool (Bilkovic et al., 2016).

### *Gaps in Research & Barriers to Implementation*

Though the ecological benefits of living shorelines (and consequences of hardening) have been well documented (Bilkovic & Mitchell, 2013; Bilkovic & Roggero, 2008; Colden et al., 2016; Gittman, Peterson, et al., 2016; Gittman, Scyphers, et al., 2016; Humphries & La Peyre, 2015; Peters, Yeager, & Layman, 2015; Scyphers, Powers, et al., 2015; Scyphers et al., 2011; Sharma et al., 2016; Theuerkauf et al., 2017), there is still a need for long term monitoring of their storm resiliency, erosion control capacity, and effect on adjacent properties (Myszewski, Alber 2016). For resource managers, policy makers, and land owners to make informed decisions related to site selection and design, much more data is needed. The lack of peer reviewed, quantitative evidence related to living shorelines is one of the largest barriers to their increased use (Bilkovic et al., 2016;

O'Donnell, 2017). There is also a need for direct comparisons of living shorelines to other forms of hard armoring, particularly in a high tidal range environment. The effects of geomorphology, hydrodynamics, and climate on the viability of both grass and oyster species used in living shorelines makes predicting the success of a living shoreline in a new location difficult, further highlighting the need for expanded data sets.

The lack of available information directly comparing various armoring methods contributes to landowner skepticism and confusion during the decision-making process, and reluctance on the part of policy makers (Scyphers, Picou, et al., 2015). Smith, et al. (Smith et al., 2017) undertook a survey of 689 North Carolina waterfront property owners, finding that landowners largely viewed bulkheads as the most effective method of erosion control, despite being more costly, requiring repairs more often, and proving more susceptible to storm damage than natural infrastructure. The study also notes that "bulkhead remediation", or the removal of hard armoring for restoration purposes or in favor of natural infrastructure rarely takes place. This highlights the urgent need for longer term datasets concerning the effectiveness of living shorelines, as well as an expedient method of communicating results to the public. It is only through a more complete understanding of their effectiveness and success that we may confidently encourage their use over hard armoring (O'Donnell, 2017).

The knowledge that landowners are unlikely to reverse an initial decision to hard-armor (or soft-armor, perhaps) has major implications for the current state of our coastline as well as its future. The first living shoreline in Georgia was permitted in 2003 by the Georgia DNR-CRD, one of thirteen that would be permitted over the following eleven years (available records ending in 2014). During that same time, some four

hundred and thirty traditional hard armoring structures were permitted. By no means would each of these sites been suitable for living shorelines, but certainly one could posit that more than 0.03% could have been candidates, had landowners been informed of their options. If, over the next ten years, the state was to increase that percentage to just *ten* percent, Georgia could boast forty to fifty living shorelines at minimum. The ecosystem services that these structures would provide are alone worth working towards such a reasonable goal, not to mention an opportunity to protect properties, save money, and build a dataset that we desperately need.

### *Structure-from-Motion as a Monitoring Tool*

The need for long term monitoring of living shorelines also highlights the lack of methods that afford both a high spatial and temporal resolution for quantifying volumetric topographic change. The current methods of choice each come with drawbacks. High spatial resolution three-dimensional data can be achieved using aerial light detection and ranging (LiDAR) or terrestrial laser scanning (TLS), the former offering large extents at a lower resolution, and the latter increasing resolution at the expense of spatial extent. Each can be cost prohibitive and labor intensive and thus limit available data (Cook, 2017; Mancini et al., 2013). Real time kinematic (RTK) GPS is a more affordable method of surveying topographic change but is labor intensive and sacrifices spatial resolution for extent (Mancini et al., 2013). In a marshland setting, physical access can also act as a barrier to data collection via ground survey. In turn, many erosional processes are poorly understood simply due to a lack of affordable methodology capable of monitoring total soil volume losses and gains (Nouwakpo et al., 2017). A lack of up-to-date three-dimensional data in coastal areas can also contribute to

a lag time in our understanding of the effects of increased development and shoreline hardening on coastal erosion and flooding. A recent study attempted to quantify coastal land loss in two dimensions based on analysis of historical aerial photos and shoreline position change, but undercutting of banks, changes in elevation, and total volume of soil lost could not be captured (Wakefield, 2016). This type of analysis is also often conducted at a spatial resolution that is too coarse to identify micro-topographical change.

Structure-from-motion (SfM) is an emerging technology that relies on collections of overlapping photos and long-held principles of photogrammetry to reconstruct three dimensional surfaces. Imagery is often acquired using an unmanned aerial system (UAS), offering a low-cost alternative to LiDAR or TLS data acquisition as well as access to hard to reach areas of coastline (Mancini et al., 2013; Papakonstantinou, Topouzelis, & Pavlogeorgatos, 2016). Even very basic UAS and cameras can be used to create detailed 3D models at both a high spatial (< 10cm) and temporal resolution (determined entirely by the UAV operator) (Cook, 2017; Dietrich, 2017; Klemas, 2015; Long, Millescamps, Guillot, Pouget, & Bertin, 2016; Long et al., 2016 b). The ease and accessibility of SfM allows for the fast acquisition of three-dimensional data over reasonably large spatial extents. SfM also differs from traditional photogrammetry in that less expertise is required and processing can be fully automated via software (Marteau, Vericat, Gibbins, Batalla, & Green, 2017). Thus, SfM offers a method of continually collecting data to observe changes in sheet erosion, preferential flow paths, deposition, and total volumetric changes. It shows particular promise in the study of fluvial geomorphology and

evaluation of restoration projects. (Cook, 2017; Marteau et al., 2017; Nouwakpo et al., 2017).

Agisoft PhotoScan, the software program used in the majority of SfM research, provides a user-friendly workflow for the creation of dense point clouds, orthomosaics, and digital surface models (DSMs). Uploaded images are automatically aligned and multiview stereo algorithms allow for the creation of an extremely dense point cloud based on image matching. GPS surveyed ground control points (GCPs) are used to register the model into a geographic coordinate system (on board UAV GPS data can be used to georeference models with surprising accuracy in the X and Y directions but has not been found to be reliable for generating elevation values). A number of tools are present within the software to reduce error and "noise" within the model as well. Following dense point cloud creation and georeferencing, one can create a textured mesh, orthophoto, or DSM for export and analysis (Cook, 2017; Marteau et al., 2017). Model precisions on the order of 1-3 mm have been achieved but are extremely reliant on a robust and accurate network of GCPs (Marteau et al., 2017; Nouwakpo et al., 2017). For the most accurate results, both horizontal and vertical coordinates of GCPs are measured using an RTK-GPS or a total station prior to image acquisition, and can be directly compared to generated point clouds as a metric of error (Cook, 2017).

To understand volumetric changes in sediment, a series of DSMs or digital elevation models (DEMs) are extracted from successive point clouds, and then compared using a DEM-of-difference method or cloud-to-cloud comparisons (Cook, 2017; Dietrich, 2017). Orthomosaics can also be created in PhotoScan and then used to assess changes in

vegetation using an image classification tool available from ESRI ArcMap (Marteau et al., 2017).

An extremely important step in the use of SfM data to assess topographic change is the determination of error to distinguish actual change from noise present in the point cloud. Marteau et al. (2017) refers to this error as the "minimum level of detection". This is achieved through direct comparison of SfM derived point clouds with either TLS or GCP point coordinates, which serve as a control. Root mean squared error (RMSE) between SfM and control points varies based on the topography being surveyed, image resolution, quantity, and overlap, and the quality of GCPs, and so can range from less than 10 cm to greater than 1 m.

Water, vegetation, and small scale topographic changes not captured by certain photo angles are often the main sources of error in a SfM derived model. The constant movement of vegetation and water can create a "smoothing", or blur, caused by difficulty in photo matching. Vegetation may also occlude the soil surface, making DEM generation difficult. To combat this problem, extreme oblique images should be used to minimize soil occlusion, or vegetation removed from the point cloud entirely based on ground surveyed stem height and elevation (Mancini et al., 2013; Nouwakpo, Weltz, & McGwire, 2016). Issues of coverage are solved by thorough photographing of the study site from multiple angles and elevations. (Cook, 2017).

Multiple SfM assessments of topographic change have been carried out in the coastal zone. (Brunier, Fleury, Anthony, Gardel, & Dussouillez, 2016; Casella et al., 2016; Hayes, Timmer, Deutsch, Ranger, & Gingras, 2017; Long, Millescamps, Guillot, et al., 2016; Long, Millescamps, Pouget, et al., 2016; Lu, 2016; Mancini et al., 2013;

Papakonstantinou et al., 2016; Turner, Harley, & Drummond, 2016; Ventura, Bruno, Lasinio, Belluscio, & Ardizzone, 2016; Yoo & Oh, 2016). However, these have largely focused on areas of exposed beach or dune formations rather coastal wetlands and have yet to address the issues of vegetation and tidal range that would be encountered in Georgia salt marshes. The work of Jaud et al. (2016) quantified sediment dynamics in a tidal mudflat using UAS imagery, identifying standing water as a challenge to SfM modeling, but did not address the issue of marsh vegetation. Possibly most applicable to the proposed research are studies in which UAS imagery has been used to track changes in fluvial geomorphology, as they address the issues of water, complex topography, erosion, and vegetation (although not high tidal range) (Brunier, Fleury, Anthony, Pothin, et al., 2016; Christian & Davis, 2016; Javernick, Hicks, Measures, Caruso, & Brasington, 2015; Marteau et al., 2017; Prosdocimi, Calligaro, Sofia, Dalla Fontana, & Tarolli, 2015). The back-barrier salt marshes of the Georgia coast present a special set of challenges to SfM technology as well as great opportunity for advancement.

### *Research Objectives*

The following research had two main objectives: first, to analyze the edge effects of living shorelines and bulkheads as well as the area of influence of each structure, and second, to assess the accuracy of the SfM method as a tool for monitoring salt marsh erosion and shoreline change.

# CHAPTER 2

# METHODS

## *Site Descriptions*

A total of six study sites - three living shorelines and three bulkheads - were included in this study. Study sites were located on Tybee Island, St. Simons Island, and Little St. Simons Island (Fig. 1). Due to the limited number of living shorelines in Georgia available for study, these sites were first identified, followed by bulkheads located in similar settings that would serve as comparison sites. Bulkheads were chosen based on similarities in soil type (map unit ID GA064/GA071), upland slope (0-4%), elevation (0-10 meters), channel

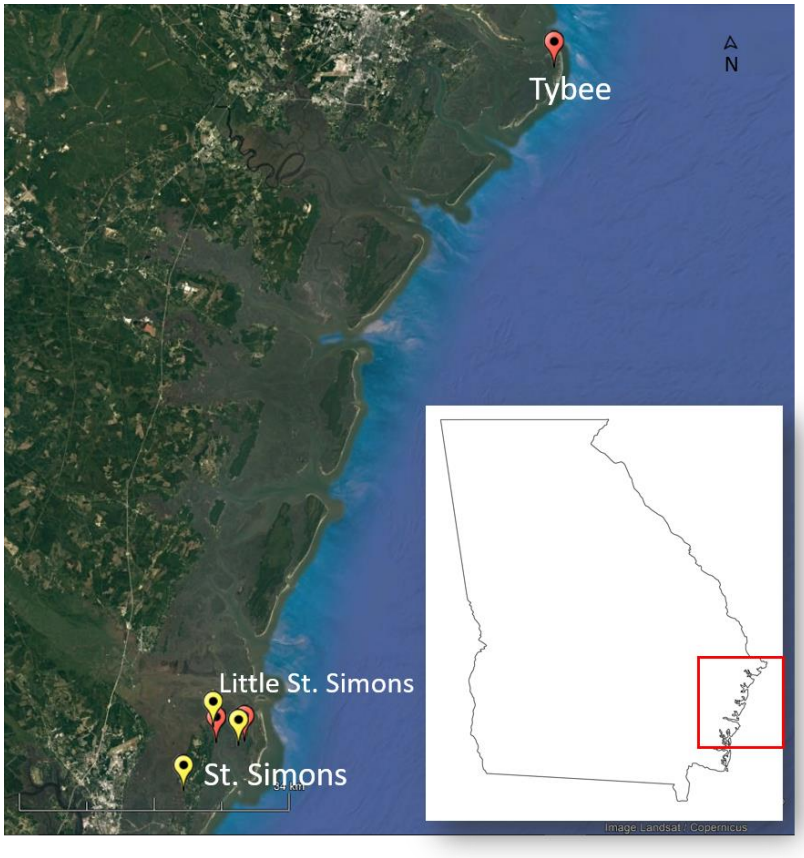


**Figure 1:** *Site locations on the coast of Southeast Georgia are pictured at left. Living shorelines are represented by a red marker, and bulkheads by a yellow marker.*

width (25-65 meters), channel depth at mean lower low water (0.5-2 .5 meters) and geomorphic setting (mid/back barrier marsh) (Table 1). The sites represent a range of upland land use, from urban to forested.

**Table 1:** *Characteristics of each study site*

| Site | Soil Type | Upland Slope | Channel Width | Channel Depth | Elevation |
|---|---|---|---|---|---|
| Tybee | GA064 | 4.0% | 25 m | 0.5 m | 0.6-0.8 m |
| Cannon's Point | GA071 | 1.0% | 30 m | 1.0 m | 1.8-5.0 m |
| LSSI Bulkhead | GA071 | 1.0% | 65 m | 1.5 m | 2.0-7.0 m |
| LSSI Living Shoreline | GA071 | 2.2% | 65 m | 1.5 m | 2.0-7.0 m |
| Dunbar Creek | GA064 | 1.0% | 63 m | 2.5 m | 2.9-4.0 m |
| Jones Creek | GA071 | 1.0% | 60 m | 2.5 m | 1.7-10 m |

***Data Acquisition***


***Figure 2:*** *The area of influence of each structure was determined by surveying the streambanks 50 meters adjacent to each structure. Stream banks adjacent to a living shoreline are indicated in red, and those adjacent to a bulkhead are indicated in yellow. Note, a bulkhead and a living shoreline are installed directly adjacent to one another at Little St. Simons, meaning only one side of each structure was surveyed at that site. While this "combination" site is unusual to the present study, it represents a situation that would likely be encountered by a landowner and was included for this reason. Upstream and downstream locations are marked "U" and "D" respectively.*

To determine the area of influence of each armoring structure, stretches of bank both 50 meters up and downstream of the structure (Fig. 2) were surveyed. using UAS and erosion pins (2 cm x 38 cm PVC pipe).

*Ground Measurements*

Erosion pins were placed at 5-meter increments along the bank, approximately 0.5 m above mean low tide and 0.5 below mean high tide. Pins were driven perpendicularly into the stream bank, leaving approximately 10 cm exposed. This was done from a kayak so as not to disturb the bank, as each bank was comprised of soft silts that would not readily support the weight of a person. The length of pin exposed was measured at the time of installation, as well as at the time of each UAS flight.

*UAS Survey*

UAS imagery was acquired at each site using a DJI Phantom 4 Pro. Flight altitude for aerial image capture was set to 60.96 meters, which afforded a ground pixel size of 2.54 cm. Aerial images were taken of each study site at an 80% end lap and 20% side lap, sufficient for creation of three dimensional models. Each flight was performed at or as close to mean low water as possible to allow for the maximum amount of exposed stream bank. Oblique imagery of each stream bank was also taken using the UAS to account for any areas of stream bank that may have been occluded in aerial images by vegetation, structures, undercutting, or scouring. This was originally taken as video, and then still images rendered using the open source software program Blender (Blender Foundation, 2017). Image acquisition at each study site (averaging five hectares) required approximately thirty minutes, and one battery pack per UAS flight. Aerial images were

acquired using an automated flight plan programmed by the Map Pilot app, and oblique videos were flown manually.

### *Data Processing*

#### *Orthophoto and Point Cloud Generation*

All imagery was initially processed using the software program Agisoft PhotoScan Professional. Images were processed in two chunks – aerial and oblique – with identical workflows for each. Images were first imported into the program, and then aligned using default settings to create a sparse point cloud (Highest accuracy, generic preselection, reference preselection, key point limit 40,000, tie point limit 4,000, adaptive camera model fitting). Each model was created using between 100-200 photos, and initial sparse clouds contained between 150,000-300,000 points. Gradual selection, a set of iterative tools within the PhotoScan software, was then used to reduce error within the sparse point cloud based on a workflow developed by the U.S. Geological Survey (USGS, 2017). Using these tools, reconstruction uncertainty was reduced to level 10, projection accuracy to level 5, and reprojection error to level 0.3. Each value relates to the accuracy of points generated by the software relative to known camera positions. Cutoff points were empirically derived by the USGS to provide the most accurate model possible. Any points falling above these cutoffs were removed from the model. This resulted in a much less dense (20-50% of original), but much more accurate point cloud. Cameras locations were then re-aligned based on these more accurate points.

Following alignment, error reduction, and any necessary manual cleanup of the sparse point cloud, a dense point cloud was created using medium quality and disabled

depth filtering settings. Medium quality was chosen to minimize processing time while maximizing detail. Dense clouds created using the highest quality settings showed no marked improvement in detail, but vastly increased processing time (on average, from 1-3 hours to 13-18 hours). Depth filtering was disabled in order to minimize smoothing of the point cloud that may have obscured detail on the stream banks. PhotoScan requires the generation of a mesh prior to a digital surface model or orthomosaic, however the quality of the mesh does not appear to impact either subsequent product and so was again built using a low setting in order to minimize processing time. Finally, an orthomosaic (2.5 cm resolution) was created and exported in the Universal Transverse Mercator (UTM – Zone 17N) coordinate system using the 1983 North American Datum (NAD83). Prior to export, models could be further georeferenced by adding ground control points with known X, Y, and Z coordinates. We explored the use of the internal UAV GPS alone as well as the addition of external GCPs in improving model accuracy and workflow efficiency, which will be discussed in later sections.

When GCPs were incorporated, they were added post-camera alignment by importing X, Y, and Z coordinates that had been identified using existing LiDAR datasets. Following their import, PhotoScan automatically places markers within each photo which were then manually refined. Camera locations were optimized once again, and a new dense point cloud was exported.

### *Horizontal Accuracy Assessment*

#### *Precision of DJI Internal GPS*

To assess the precision of the DJI internal GPS from one imagery acquisition to another, ten ground control points were first identified in each orthomosaic. Immobile features such as docks, buildings, sidewalks, and roads that were visible in both sets of imagery were chosen to serve as GCPs. If such features were not well distributed throughout the orthomosaic, small upper-marsh channels were used in some cases, as these channels have been shown to remain stable over long time periods (Redfield, 1972). Residuals, or the measured difference between the same point in two mosaics, were measured in ArcGIS using the point distance tool. These values were then used to calculate the combined XY root mean squared error (RMSE) as follows, where P equals the predicted XY value and O equals the observed XY value:

$$\mathrm{RMSE} = \sqrt{\frac{\sum_{i=1}^{n} \left(P_i - O_i\right)^2}{n}}$$

*Accuracy of DJI Internal GPS*

To determine the relative accuracy of orthomosaics derived from the DJI internal GPS as compared to 2012-2013 NOAA 15.24 cm (6-inch) resolution orthoimagery (accuracy +/- 0.762 m/2.5 ft), the same process was repeated, this time comparing each orthomosaic to a corresponding NOAA orthophoto. RMSE was again calculated for both the X, Y, and combined X/Y directions. In one

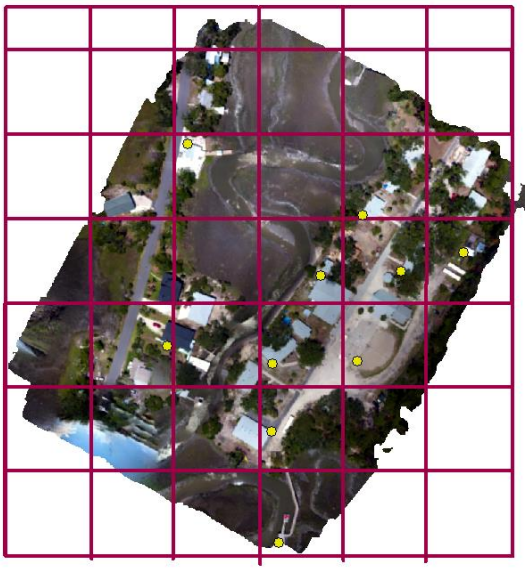

***Figure 3****: Sampling grid overlaid upon a UAS derived orthophoto, with QC points shown in yellow.*

instance (Cannon's Point Preserve), significant construction had occurred after the 2012 imagery was acquired, rendering four of the ten ground control points unusable. Thus, only six GCPs were used when comparing Cannon's Point to NOAA imagery. This did not appear to affect the final result.

The same NOAA imagery was then used to georeference each orthomosaic in the interest of increasing accuracy using freely available satellite imagery. The ten identified ground control points were referenced to the NOAA imagery in ESRI ArcMap, and the X and Y RMSE for each GCP calculated by the software. Ten additional quality control points were randomly selected in each orthomosaic, and the RMSE calculations repeated in order to determine the effect of georeferencing on the orthomosaic as a whole. This was done by overlaying a grid of 50-m by 50-m squares onto the image and using a random number generator to locate grid squares to be sampled (Figure 3). Within each grid square, a fixed feature such as a building, road, or sidewalk was identified to use as a quality control point. In the event that no such feature was identifiable in the chosen grid square, nor was a stable creek channel, a new square was randomly selected until a total of ten quality control points had been identified.

*DSM Generation and Erosion Calculation*

Surface models were generated in ArcMap using georectified dense point clouds created in PhotoScan. Point clouds derived from the UAS internal GPS alone were not used in any analysis due to the overwhelming error in Z values.

Following import into ArcMap, clouds were then rasterized to produce 10 cm resolution digital elevation models representing each data acquisition. Ten-cm resolution

was chosen based on the upper limit point spacing of all point clouds. This is done using the LAS Dataset to Raster Tool in ArcGIS. The output of this tool is a gridded dataset, each cell containing a discrete X, Y, and Z value. Following DSM generation, each raster was clipped to represent only exposed streambank, excluding any water of vegetation that might increase error in the analysis. The Raster Calculator tool was then used to subtract one clipped DSM from another, providing an analysis of the elevation change that occurred in each 10 cm cell over time. The resulting product, a "DSM of Difference", provides a heat map of erosion and deposition throughout each study area streambank. Zonal statistics were then calculated for the upstream and downstream areas, as well as in five-m increments at one bulkhead and one living shoreline site in order to determine an area of influence.

### *Relative Vertical Accuracy Assessment*

To determine the accuracy of each DSM as a whole, a DSM of difference calculation was performed on the entire site comparing each data collection time to another—pre-Irma to post, post-Irma to post-season, and pre-Irma to post-season. Quality control points were then identified on flat surfaces distributed throughout each site (including pavement, grass, and high marsh with little vegetation). It was assumed that these locations should remain largely unchanged from one model to another, and so any difference between the two should be considered noise or a "minimum detection level". The elevation differences between each of these points was then extracted to a table using the ArcMap Sample tool, and an RMSE calculated for each site.

### *Historical Trend Analysis*

***Table 2:*** *Installation years and imagery used for pre and post armoring installation trend analysis. USDA NAIP imagery was used when available (generally 2009 and later). This imagery is acquired at a ground resolution of 1-meter with a horizontal error of 6 meters. Single aerial photos were used for analysis of earlier years and were georeferenced to NAIP imagery. All imagery was acquired via USGS Earth Explorer.*

| Location | Installation Year | Imagery Used |
|---|---|---|
| Tybee Island Living Shoreline | 2015 | Pre: 1951, 1971, 1994, 2009<br>Post: 2015, 2017 |
| Cannon's Point Living Shoreline | 2015 | Pre: 1951, 1974, 1993, 2013<br>Post: 2015, 2017 |
| LSSI Living Shoreline | 2013 | Pre: 1951, 1974, 2010<br>Post: 2013, 2017 |
| LSSI Bulkhead | 1995 | Pre: 1951, 1974, 1984<br>Post: 1984, 2007, 2017 |
| Dunbar Creek Bulkhead | 1985 | Pre: 1951, 1974, 1982<br>Post: 1982, 2007, 2017 |
| Jones Creek Bulkhead | 1982 | Pre: 1951, 1974, 1982<br>Post: 1982, 1993, 2013, 2017 |

Processes of erosion and deposition occur on multiple temporal scales, and so to gain an understanding of the long-term trends present at each study site, a historical analysis of shoreline position change was performed on the areas 50 m upstream and downstream of each structure. This was done using AMBUR, a package developed for

the open sourced software R (Jackson, Alexander, & Bush, 2012). AMBUR (Analyzing Moving Boundaries Using R) employs a multiple transect method to calculate gains and losses in shoreline position over time. This allowed for a more holistic view of the behavior of each study site both before and after the installation of armoring. The earliest available imagery via USGS Earth Explorer (1951) was used as a starting date. (Table 2)

# CHAPTER 4

# RESULTS & DISCUSSION

## *Horizontal Accuracy*

Orthomosaics derived from successive UAS flights were found to have a combined XY precision of 2.27 meters using the UAS internal GPS alone. Highest mean precision was observed at Little St. Simons Island (1.65 m) and lowest at Cannon's Point Preserve (2.95 m). When compared to 6 inch/15.24 cm resolution NOAA aerial imagery, orthomosaics derived using the UAS internal GPS had a mean XY accuracy of 1.97 meters. The highest XY accuracy was found at Jones Creek (1.57 m), and the lowest at Tybee Island (2.39 m). It should be noted that there exists an inherent +/- 0.762-meter error in the NOAA imagery. This implies that the images are likely more precise in relation to one another than they are accurate with respect to NOAA imagery. If one's research need was relative change detection alone, the most accurate product may be derived from georectifying successive images to *each other* rather than to a separate data set with additional inherent error. As it is not likely that one would create a dataset that was never intended to be used in conjunction with another, it is then of utmost importance to take into account the inherent error of the base data used for rectification. This should be kept in mind when viewing the following results, each of which carry an associated error of +/- 0.762 m (Table 3).

Following georectification to NOAA aerial images, accuracy of ground control points (GCPs) was reduced to a mean of 20 centimeters for all sites. The lowest GCP accuracy was found at Dunbar Creek (25 cm) and the highest at Cannon's Point Preserve (9 cm). It is important to note that these acuuracy values correspond to the GCP locations alone, and do not reflect the accuracy of the orthomosaic as a whole. Assessing the accuracy of additional quality control (QC) points throughout the mosaic is essential to determining the accuracy of the entire image. Significant warping may occur at the edge of each mosaic or may result from poor distribution of ground control points, causing the image to distort or stretch to accommodate georectification. QC points distributed throughout each mosaic were found to have a mean XY accuracy of 1.07 meters. Despite having the most accurate GCPs, Cannon's Point Preserve was the least accurate in terms of QC points at 1.29 m. The most accurate was Tybee Island at 82 cm.

The first three metrics (precision, absolute accuracy, and GCP RMSE) did not appear to follow a trend; however, the accuracy of QC points seems closely related to the number and distribution of identifiable cultural features in the image. These features, such as buildings, sidewalks, and crossroads, allowed for a much more uniform and accurate georectification. Those locations without well distributed cultural features for georectification (Little St. Simons Island and Cannon's Point Preserve) were subject to more distortion.

Though these horizontal accuracy values may not suffice for all studies, they show great promise for those whose research occurs at a coarse spatial resolution or large temporal scale. There are countless questions that can be addressed within a horizontal error margin of two meters or less, an easily achievable goal using the UAS method.

***Table 3**: Mean, maximum, and minimum (both in red) horizontal error values of orthomosaics derived from UAS imagery. Column one addresses the precision of successive UAV flights to one another, while columns two through four relate UAV derived imagery to NOAA aerial imagery (+/- 0.762 meters horizontally).*

| | Precision RMSE (m) | Accuracy RMSE(m) | GCP RMSE (m) | QC RMSE (m) |
|---|---|---|---|---|
| Cannon's Point | 2.95 | 1.91 | 0.09 | 1.29 |
| Dunbar Creek | 2.03 | 1.80 | 0.25 | 1.13 |
| Jones Creek | 1.81 | 1.57 | 0.24 | 1.24 |
| LSSI | 1.65 | 2.17 | 0.22 | 0.89 |
| Tybee | 2.90 | 2.39 | 0.20 | 0.82 |
| **Mean** | **2.27** | **1.97** | **0.20** | **1.07** |
| *Std. Err.* | *0.15* | *0.11* | *0.05* | *0.09* |

***Vertical Accuracy***

Digital surface models derived from UAV point clouds were found to have a mean vertical precision of 0.58 meters. Tybee Island proved the most precise with a mean vertical accuracy of 0.06 m, while Jones Creek was the least with a mean vertical accuracy of 1.60 m (Table 4). As with previous horizontal error values, the vertical errors below must be considered in conjunction with the inherent error of the base data used for georectification. Both datasets (NOAA Coastal LiDAR and Glynn County LiDAR) carry an associated vertical error of +/- 0.15 cm.

The most precise site, Tybee Island, likely benefited from an abundance of open, flat surfaces with which to georectify. Seasonal changes, as well as the challenge of

penetrating dense marsh grass with LiDAR create obvious issues when attempting to standardize elevations from one point cloud to the next. The Jones Creek site was somewhat of an anomaly. While many cultural features and open, flat areas were available as rectification points, the area was also subject to damage during Hurricane Irma and saw considerable construction and landscape change throughout the study. This change contributed to a high level of vertical error and should be taken into account in future studies. Each of the following RMSE values should be considered a minimum level of detection when viewing elevation change data.

***Table 4:*** *Mean, maximum, and minimum (both in red) vertical accuracy values of digital surface models derived from UAS imagery. Each were georectified to NOAA or Glynn County aerial LiDAR (+/- 0.15m)*

| **Location** | **Precision RMSE (m)** |
|---|---|
| Cannon's Point | 0.26 |
| Dunbar Creek | 0.33 |
| Jones Creek | 1.60 |
| LSSI | 0.62 |
| Tybee | 0.06 |
| **Mean** | **0.58** |
| *Std. Err.* | *0.15* |

### *Historic Shoreline Change*

Following AMBUR analysis of the areas adjacent to each structure using aerial photography spanning from 1951 through 2017, study sites did not display significant differences in shoreline change rate following the installation of an armoring structure. It is useful, however, to view seasonal erosion data through the lens of a larger trend. In addition to mean change rates and standard deviation, the following data include a mean

error (ME) value. An X/Y error value has been assigned to each data point based on the accuracy of base data used for analysis, and ME represents the mean X/Y error across all points. Graphed error bars (Figures 4-7) are specific to each data point.

Cannon's Point Preserve experienced a mean annual change rate of -0.002 meters per year (SD=0.18, ME=0.50) prior to the installation of a living shoreline, and a change rate of -1.20 m/yearr (SD=0.45, ME=4.24) post-installation, however this difference was not significant at p=0.07. Additionally, analysis of post-living shoreline changes was performed on time spans of 3-5 years versus fifty or more pre-installation, contributing to increased error values in post-installation data.

Tybee Island underwent erosion at a rate of -0.16 m/year (SD=0.19, ME=0.33) prior to living shoreline installation and has continued to erode at a rate of -0.87 m/year (SD=0.45, ME=4.24). Again, these differences were not significant, p=0.242. The Tybee Island site was notable in that it underwent the most change in channel morphology compared to other study sites, all of which remained relatively stable in terms of channel path. A series of orthophotos showing the changes in path that the Tybee site has undergone can be found in the Appendix I.

The area adjacent to the Little St. Simons living shoreline was accreting at a rate of 0.15 m/year (SD=0.14, ME=4.24) prior to installation, while the area adjacent to the bulkhead was accreting at a rate of 0.21 m/year (SD=0.34, ME=0.34). Post-bulkhead installation, the downstream area has eroded at a rate of -0.04 m/year (SD=0.07, ME=0.24). Post-living shoreline installation, the upstream area has eroded at a rate of -0.22 m/year. Neither change is significant, with a pre/post bulkhead p-value of 0.41 and a pre/post living shoreline p-value of 0.59. It should be noted that Little St Simons Island is

subject to considerable boat traffic, which likely contributes to erosion both up and downstream. As stated before, all living shoreline sites were installed post-2013. Thus, each post-installation analysis includes two major hurricanes in a three to five-year time span. This should also be considered when viewing trends.

Dunbar Creek experienced accretion of 0.03 m/year (SD=0.18, ME=0.27) prior to bulkhead installation and erosion at a rate of -0.28 m/year (SD=0.20, ME=0.25) following armoring. These were also statistically insignificant, p=0.24.

Finally, Jones Creek underwent erosion upstream of the eventual bulkhead location prior to installation at a rate of -0.15 m/year (SD=0.03, ME=0.27) and accreted upstream following bulkhead construction at 0.04 m/year (SD=.06, ME=0.25). Downstream shoreline change was not calculated at this site due to occlusion by trees. This site revealed the most difference pre and post construction but was still insignificant at p=0.06.

Mean upstream and downstream annual change rates for each group can be viewed in the figures below. It is interesting to note that none of the study sites were eroding at a significant rate prior to armoring installation, however this analysis was performed on the adjacent areas rather than the armored locations themselves.

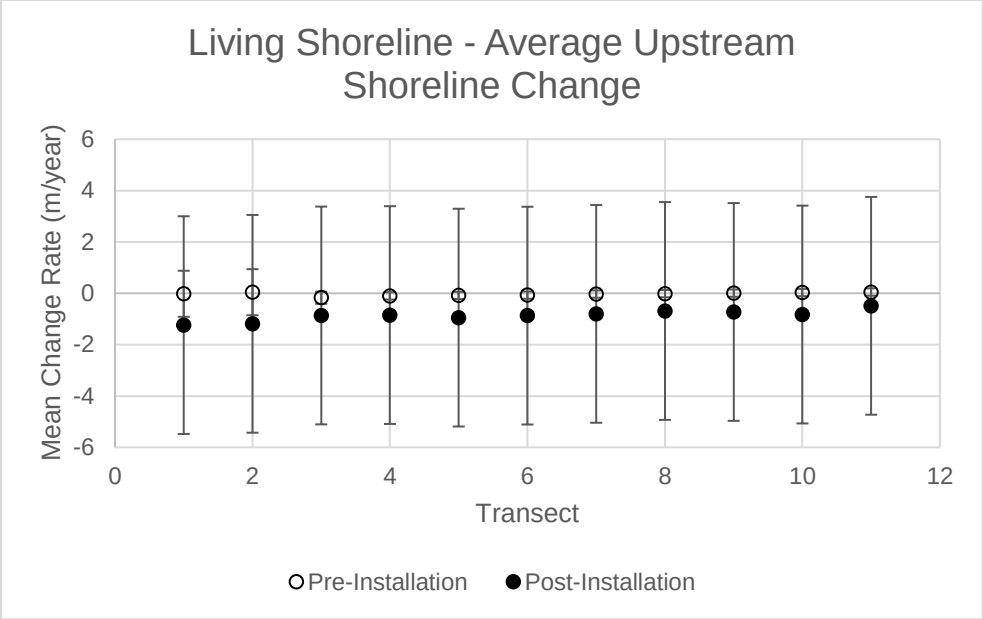


***Figure 4:*** *Average annual change upstream of living shorelines*

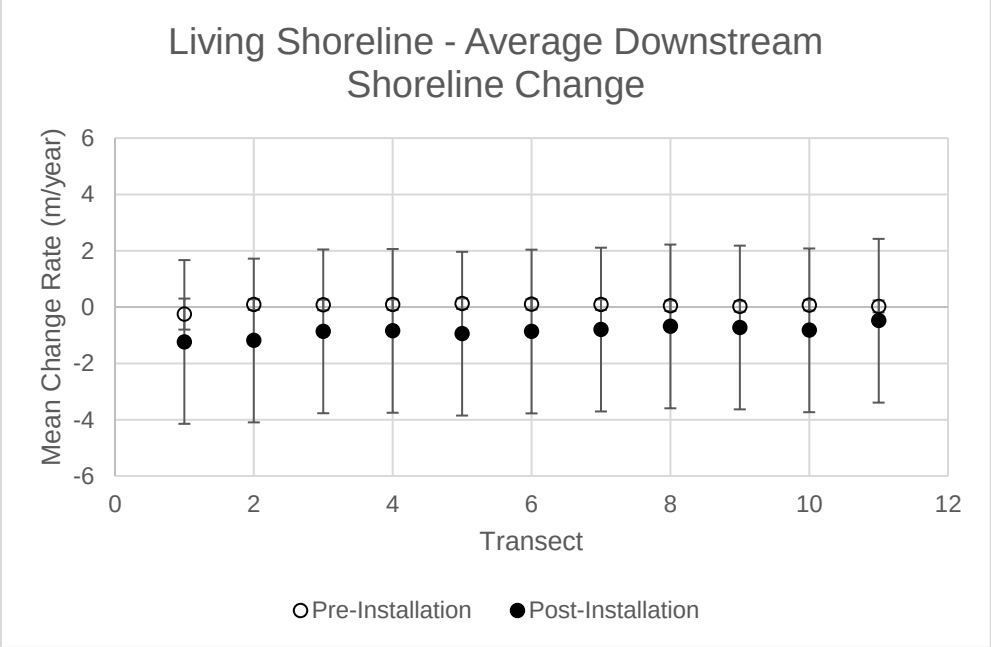


***Figure 5:*** *Average annual change downstream of living shorelines*

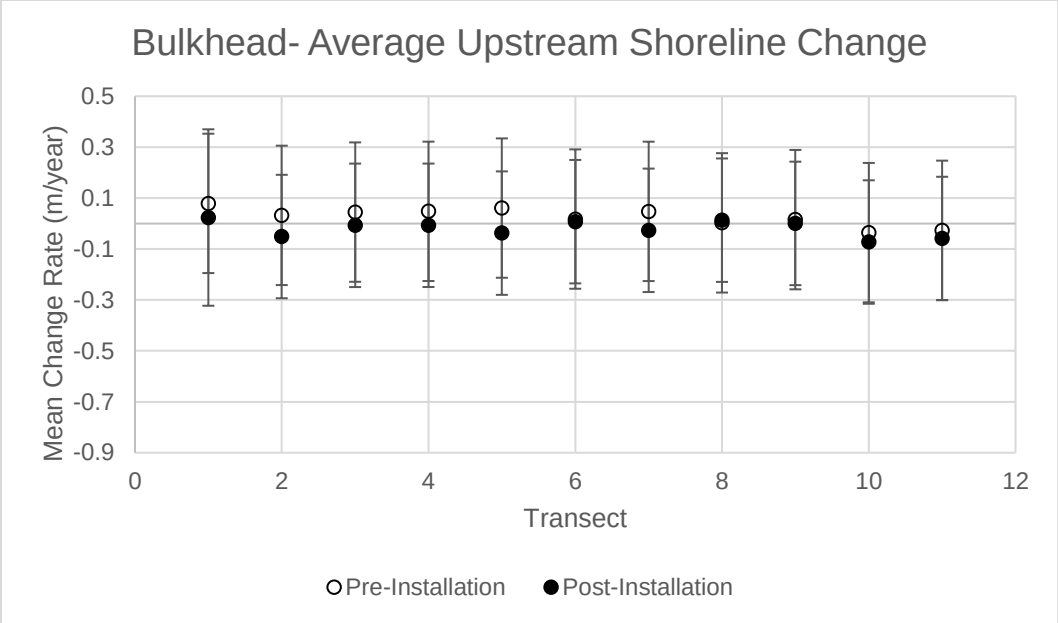


***Figure 6:*** *Average annual change upstream of bulkheads*

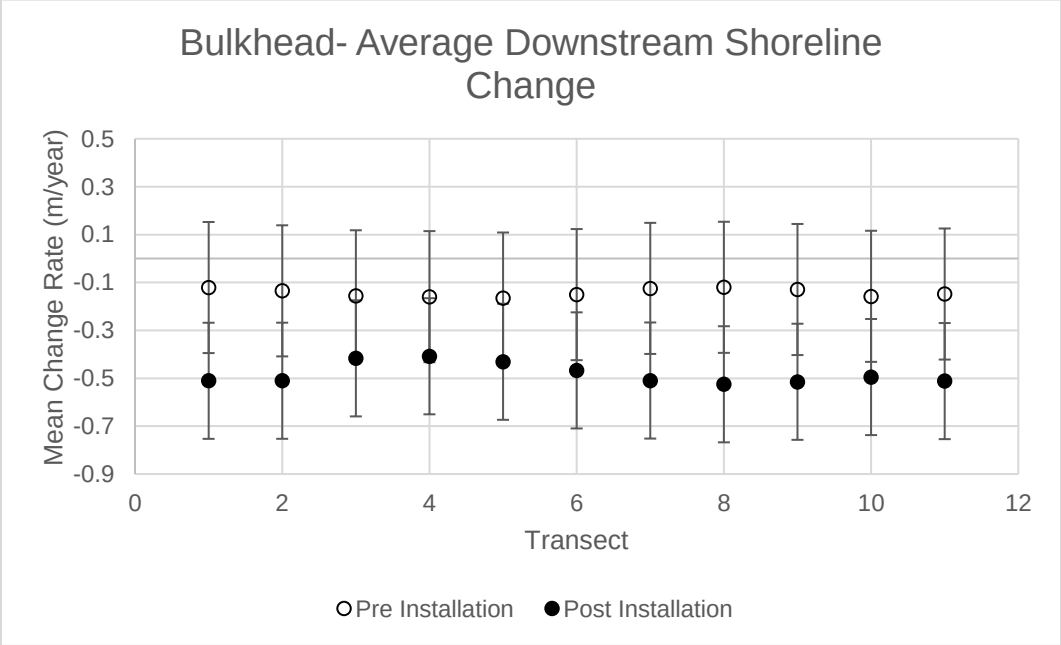


***Figure 7:*** *Average annual change upstream of bulkheads*

***Figures 4-7:*** *Mean annual shoreline change rates in the areas 50m upstream and downstream from shoreline armoring structures. Pre and post-installation rates are presented. Note that living shorelines carry a much larger error due to their age and the limited data available to assess post-installation change.*

### *Erosion Pins*

Erosion pins were included as a method of ground truthing remotely sensed data. However, they proved to be much too coarse in resolution to provide meaningful quantitative information. Many pins were either lost to erosion or buried beneath failing banks or significant sediment deposition following Hurricane Irma, leaving no data points to be observed at all. Those that did remain did not capture the highly heterogeneous nature of change at each location but did follow similar trends as those observed via remotely sensed data. A broader discussion of the data acquired via erosion pin versus UAS follows in later sections, but it should be noted that many remotely sensed data points are one order of magnitude larger or smaller than their corresponding erosion pin measurements. However, lacking high precision GPS points for each pin, it is difficult to truly compare the two. Future studies would benefit from surveying the location of each pin via RTK-GPS, however this would have to be done by boat. The use of larger diameter erosion pins would also aid in identifying them in UAS photos.

None the less, the value of on-the-ground, in person measurements at each site cannot be overstated. Though the actual data gained from these pins may not be exceptionally useful, the days and hours spent in each creek, closely observing changes with each measurement provided invaluable and intimate knowledge of the study sites, each with their own idiosyncrasies. No matter the accuracy of remotely sensed data in a quantitative sense, it should not be used without a firm understanding of the landscape being observed. Even the *most* accurate data requires interpretation by the user. A good map is most effective when it is not only seen, but remembered – the smell, sounds, and feeling of a place guiding your eye to recognize patterns in the image. It is still

recommended that erosion pins be employed in future studies as a ground truthing method, but surveyed via RTK-GPS, driven much deeper into each bank, and made from a material that will offer more visibility in the final imagery. The data that follows is frustratingly incomplete, but its collection bore countless observations, questions, and ideas, however anecdotal they may be (Figures 8-12).

A clear trend was not evident in the data collected from erosion pins, and so has been presented below in its raw form. Points of accretion have been marked in green, and points of erosion in red. Maximum points of each have been noted with an asterisk on a site by site basis. Pins have been distinguished as high or low tide, indicated by "H" or "L" in each table. The number of pins lost at the high tide line versus the low tide line was similar at each site, though the driving factors at each tidal level are likely different. Salt marsh creeks are known to experience scour beneath the roots of *Spartina,* followed by mass bank failures. This leads to the hypothesis that high tide pins were lost to mass failures, while low tide pins were buried beneath sediment accumulating on top of them.

| Jones Creek Bulkhead | Upstream Change (cm) | | | Downstream Change (cm) | | |
|---|---|---|---|---|---|---|
| | Post-Irma | Post-Season | Tidal Ht. | Post-Irma | Post-Season | Tidal Ht. |
| **0-5 m** | **3.5** | ND | H | ND | ND | H |
| **5-10 m** | ND | ND | L | **4.5*** | ND | L |
| **10-15 m** | **3** | ND | H | **-6.5*** | **4** | H |
| **15-20 m** | **3.5** | ND | L | ND | ND | L |
| **20-25 m** | **-1.5** | ND | H | ND | ND | H |
| **25-30 m** | **-1** | ND | L | **-1** | ND | L |
| **30-35 m** | **-1.5** | ND | H | **-1** | ND | H |
| **35-40 m** | **-2.5** | ND | L | **-3.5** | ND | L |
| **40-45 m** | **-5.5** | ND | H | **4.5*** | ND | H |
| **45-50 m** | **-3** | ND | L | **1** | ND | L |

***Figure 8:*** *Jones Creek erosion pin data. Nine pins were lost at low tide and ten at high tide. The only remaining high tide pin measured net erosion.*

| Dunbar Creek Bulkhead | Upstream Change (cm) | | | Downstream Change (cm) | | |
|---|---|---|---|---|---|---|
| | Post-Irma | Post-Season | Tidal Ht. | Post-Irma | Post-Season | Tidal Ht. |
| **0-5 m** | 5.5 | ND | L | -4 | ND | H |
| **5-10 m** | ND | ND | H | ND | ND | L |
| **10-15 m** | 8.5 | ND | L | ND | ND | H |
| **15-20 m** | ND | ND | H | -6* | ND | L |
| **20-25 m** | 4 | ND | L | 12 | ND | H |
| **25-30 m** | 4 | ND | H | 7 | ND | L |
| **30-35 m** | ND | ND | L | 8.5 | ND | H |
| **35-40 m** | -3.5 | 13.5* | H | -2.5 | ND | L |
| **40-45 m** | 5.5 | -1.5 | L | ND | ND | H |
| **45-50 m** | ND | ND | H | ND | ND | L |

***Figure 9:*** *Dunbar Creek erosion pin data. Nine pins were lost at both high and low tide. The remaining high tide and low tide pin measured net accretion.*

| Tybee Living Shoreline | Upstream Change (cm) | | | Downstream Change (cm) | | |
|---|---|---|---|---|---|---|
| | Post-Irma | Post Season | Tidal Ht. | Post-Irma | Post Season | Tidal Ht. |
| **0-5 m** | ND | ND | H | 8* | -10.5 | H |
| **5-10 m** | 7.5 | -4 | L | 8* | -7 | L |
| **10-15 m** | 4.5 | 4 | H | -0.5 | -5 | H |
| **15-20 m** | 0.5 | ND | L | -6.5 | ND | L |
| **20-25 m** | -11 | ND | H | -0.5 | ND | H |
| **25-30 m** | 2 | -14* | L | ND | ND | L |
| **30-35 m** | -5.5 | ND | H | -0.5 | ND | H |
| **35-40 m** | ND | ND | L | -4 | ND | L |
| **40-45 m** | -4.5 | ND | H | ND | ND | H |
| **45-50 m** | ND | ND | L | 1 | ND | L |

***Figure 10:*** *Tybee Island erosion pin data. Seven pins were lost at both high and low tide. Two of the remaining high tide pins measured net erosion and one net measured net accretion, while the remaining low tide pins experienced the opposite. Two underwent net accretion and one net erosion.*

| LSSI Hybrid | Upstream Change (cm) (LS) | | | Downstream Change (cm) (BH) | | |
|---|---|---|---|---|---|---|
| | Post-Irma | Post Season | Tidal Ht. | Post-Irma | Post Season | Tidal Ht. |
| 0-5 m | 1.5 | -1.5 | L | -2 | -0.5 | H |
| 5-10 m | ND | ND | H | -7 | 5 | L |
| 10-15 m | -10.5 | ND | L | ND | ND | H |
| 15-20 m | 1.5 | ND | H | -4.5 | 2 | L |
| 20-25 m | ND | ND | L | ND | ND | H |
| 25-30 m | 3.5 | -12 | H | -3 | -2 | L |
| 30-35 m | -9.5 | -5 | L | 8* | ND | H |
| 35-40 m | -11.5 | ND | H | 6 | -10.5 | L |
| 40-45 m | -20* | ND | L | 0.5 | ND | H |
| 45-50 m | ND | ND | H | ND | ND | L |

***Figure 11:*** *LSSI erosion pin data. Four high tide pins and one low tide pin were lost adjacent to the bulkhead. Adjacent to the living shoreline, four high tide and three low tide were lost. All remaining pins experienced net erosion.*

| Cannon's Pt. Living Shoreline | Upstream Change (cm) | | | Downstream Change (cm) | | |
|---|---|---|---|---|---|---|
| | Post-Irma | Post Season | Tidal Ht. | Post-Irma | Post Season | Tidal Ht. |
| 0-5 m | | -3.5 | H | | -5 | H |
| 5-10 m | | -9* | L | | ND | L |
| 10-15 m | | 3.5 | H | | -1 | H |
| 15-20 m | | -6.5 | L | | -2 | L |
| 20-25 m | | -2 | H | | ND | H |
| 25-30 m | | -3 | L | | -1 | L |
| 30-35 m | | 1.5 | H | | 3 | H |
| 35-40 m | | 10 | L | | 13* | L |
| 40-45 m | | 2.5 | H | | -6.5 | H |
| 45-50 m | | ND | L | | ND | L |

***Figure 12:*** *Cannon's Point erosion pin data. One high tide pin was lost and three low tide.*

***Figures 8-12:*** *Measurements taken from erosion pins placed at five-meter increments up and downstream from each streambank. Points of erosion are highlighted in red, and points of accretion in green. "ND" represents points of no data where pins were either lost to erosion or hidden under extreme deposition. Post-Irma data is not available for Cannon's Point as permits to install pins were not available at that site prior to the hurricane.*

### *Remotely Sensed Erosion*

Heat maps depicting elevation changes at each site (a proxy for erosion and accretion) immediately following Hurricane Irma, post-hurricane season (recovery from Irma), and throughout hurricane season (pre-Irma to post-season) are provided below and will be discussed individually (Figures 13-25). Water levels at Little St. Simons remained too high immediately following Irma to capture the stream bank in UAS imagery, so only data from the entire season are presented at that site. Marked differences in upstream versus downstream changes were apparent at most sites and will also be discussed separately. Change at each site should be considered in conjunction with the associated vertical accuracy, listed with each. This is considered the minimum level of detection and values falling within this range may be due to inherent noise between the two DSMs.

Cannon's Point, Dunbar Creek, and Jones Creek experienced accretion immediately following Hurricane Irma, while Tybee Island underwent erosion (data for LSSI not available). Post-Irma accretion likely resulted from an influx of sediment carried by the hurricane's storm surge, which measured four feet above the predicted high tide at the Fort Pulaski tidal gauge station. In the months following hurricane season, all sites experienced erosion. This could be caused by a of a number of factors, but Irma's disturbance of marsh vegetation that is so essential to holding sediment in place likely played a role. Quantitative before and after vegetation data would be necessary to confirm this hypothesis. The season-long cumulative effect was erosive at two bulkheads and one living shoreline, and accretive at two living shorelines and one bulkhead. These differences, however, were not found to be statistically significant at any point throughout the seasons (Table 5). It should be noted that the Jones Creek data were

extremely variable, likely due to georectification issues. These data points should be viewed with less weight than others and likely lead to skewing of the overall bulkhead data.

***Table 5:*** *Mean changes in elevation by site, as well as living shoreline and bulkhead group means. Standard deviation is presented as a means to convey variability in each dataset, P values and 95% confidence values comparing the two structure types can be seen at the base of the table.*

| | **Post Irma** | St. Dev. | **Post Season** | St. Dev. | **Entire Season** | St. Dev. |
|---|---|---|---|---|---|---|
| **Tybee** | -0.42 | 0.40 | -0.05 | 0.31 | -0.51 | 0.42 |
| **Cannon's Point** | 0.44 | 0.39 | -0.39 | 0.25 | 0.05 | 0.38 |
| **LSSI LS** | n/a | n/a | n/a | n/a | 0.01 | 0.30 |
| ***Mean*** | ***0.01*** | | ***-0.22*** | | ***-0.15*** | |
| **Dunbar Creek** | 0.39 | 0.40 | -0.06 | 0.46 | -0.58 | 0.72 |
| **Jones Creek** | 1.43 | 2.75 | -0.01 | 0.15 | 1.86 | 2.79 |
| **LSSI Bulkhead** | n/a | n/a | n/a | n/a | -0.49 | 0.47 |
| ***Mean*** | ***0.91*** | | ***-0.04*** | | ***0.26*** | |
| **p** | 0.31 | | 0.39 | | 0.64 | |
| **CI.95** | -3.80,2.00 | | -0.92, 0.55 | | -2.68, 1.86 | |

### *Tybee Island Living Shoreline - Accuracy 0.06 m*

The living shoreline at Tybee Island was the only site to undergo erosion at every data collection point, the cumulative effect mimicking that of two bulkhead sites—Dunbar Creek and Little St. Simons. The Tybee island living shoreline is also the most urbanized of all sites and likely subject to the most stormwater runoff, a known driver of erosion in urban streams. Even so, localized sediment deposition can be seen in the area immediately downstream of the living shoreline.

***Cannon's Point Living Shoreline – Accuracy 0.26 m***

Cannon's Point may serve as the most likely candidate for a "reference condition" in this study, as it is in a low traffic, low development setting. This site experienced an influx of sediment with the arrival of Hurricane Irma that was slowly removed throughout the following months. The cumulative effect at Cannon's Point was one of relative equilibrium.

***Little St. Simons Bulkhead & Living Shoreline – Accuracy 0.62 m***

As previously stated, water levels following Hurricane Irma prevented shoreline change analysis Post-Irma or Post-Season. However, a cumulative analysis was possible. The bulkhead site at LSSI underwent erosion, while the living shoreline remained at equilibrium. This site is subject to significant boat traffic however, particularly at the bulkhead site, and are a likely contributor to the increases in erosion that were observed.

***Jones Creek Bulkhead – Accuracy 1.60 m***

Analysis of the Jones Creek site poses a special set of problems not only due to the inherent error in the data, but also due to occlusion of the bank by trees and vegetation. Particularly on the downstream side of the bulkhead, the streambank was shaded so significantly that PhotoScan was not able to identify points. Significant points of scour observed immediately adjacent to both ends of the bulkhead are not visible in remotely sensed data due to occlusion by trees.

***Dunbar Creek Bulkhead – Accuracy 0.33 m***

Dunbar Creek experienced the same effect as Cannon's Point—deposition from Irma, followed by erosion, however the cumulative effect was erosive. Points of scour at adjacent to the bulkhead, particularly downstream, can be seen in both the Post-Irma and Post-Season maps.


***Figure 13**: Changes in Tybee Island streambank elevation post-Irma*

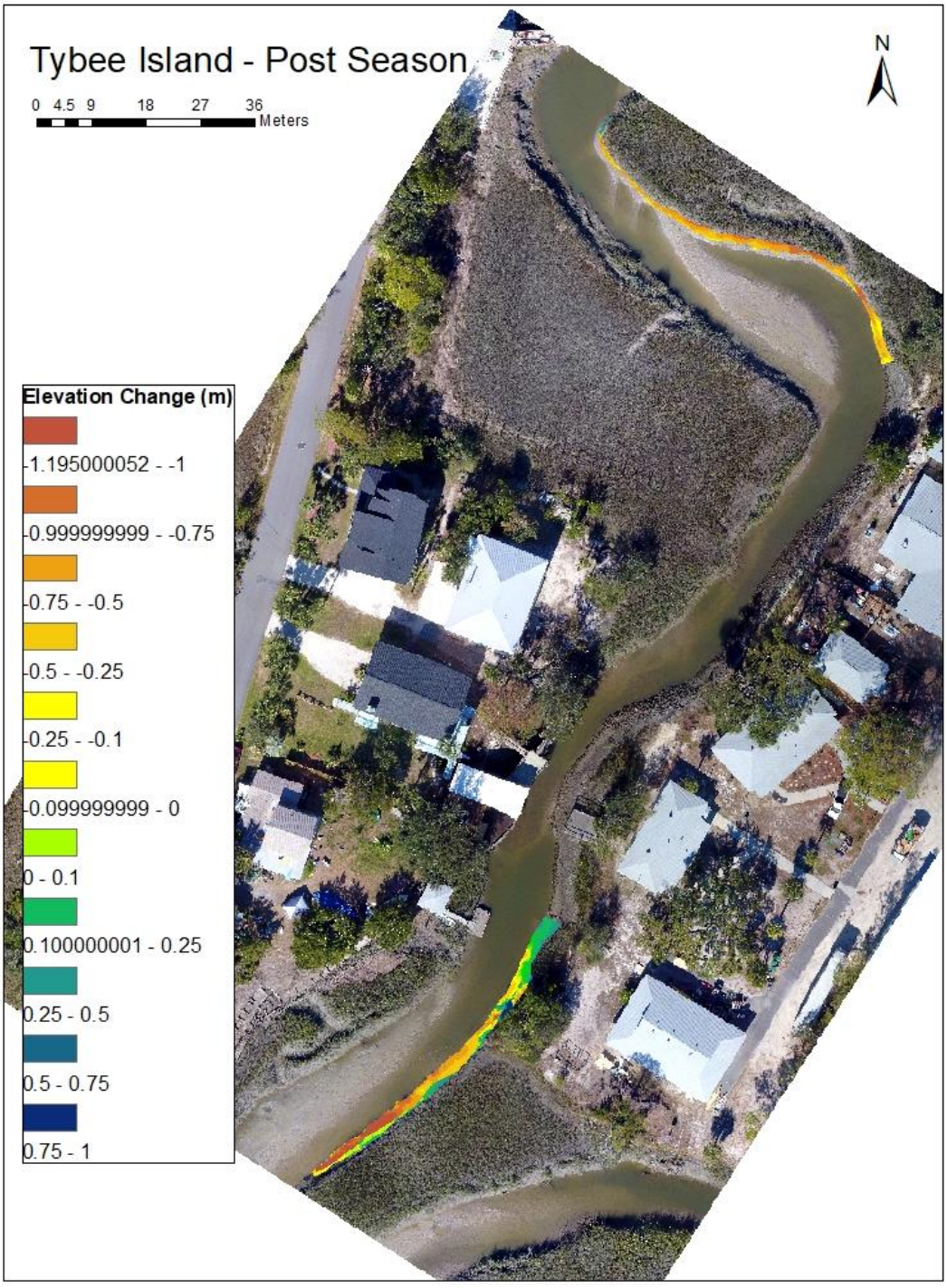


***Figure 14**: Changes in Tybee Island streambank elevation post-season*

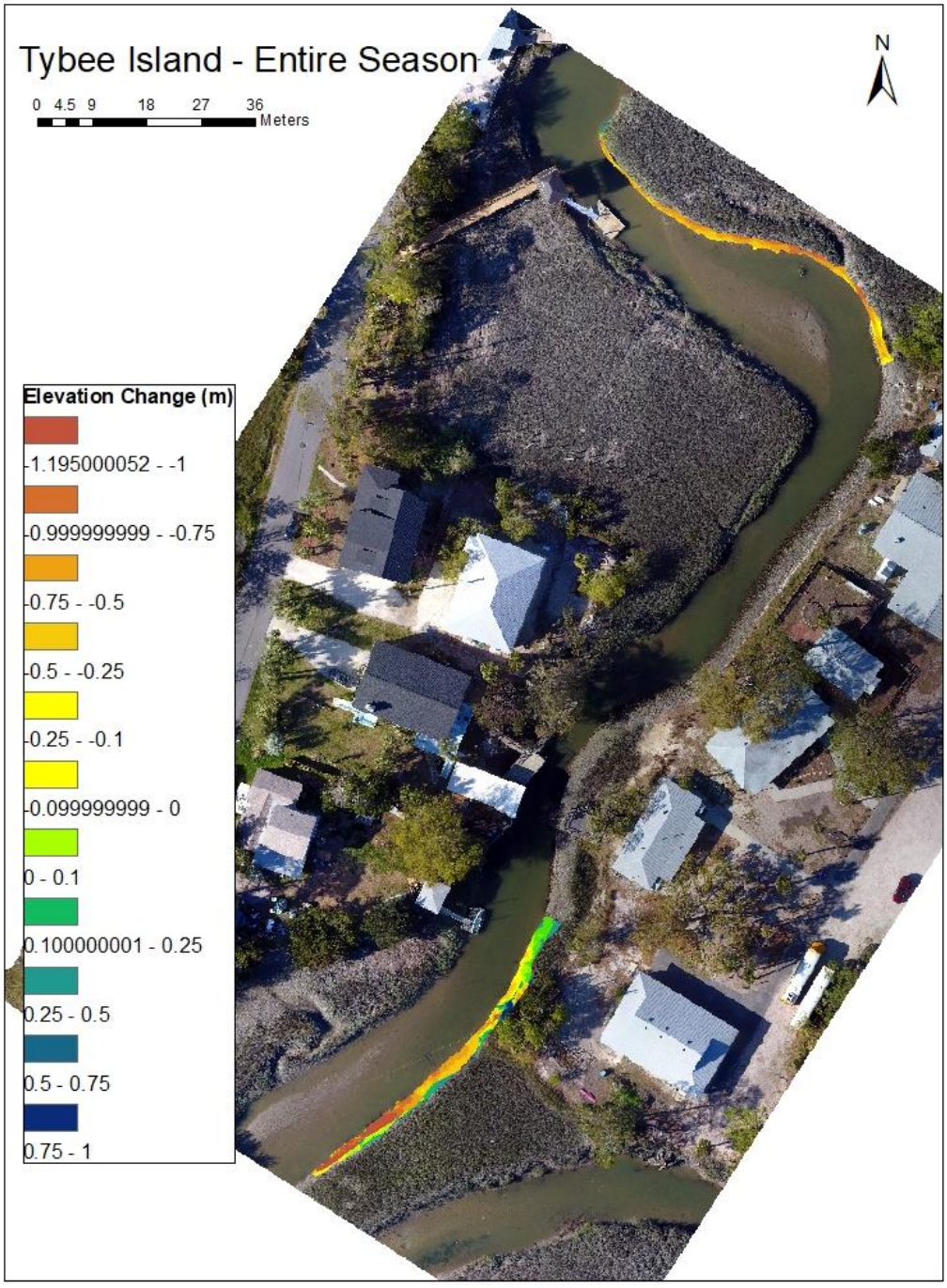


***Figure 15**: Cumulative changes in Tybee Island streambank elevation*

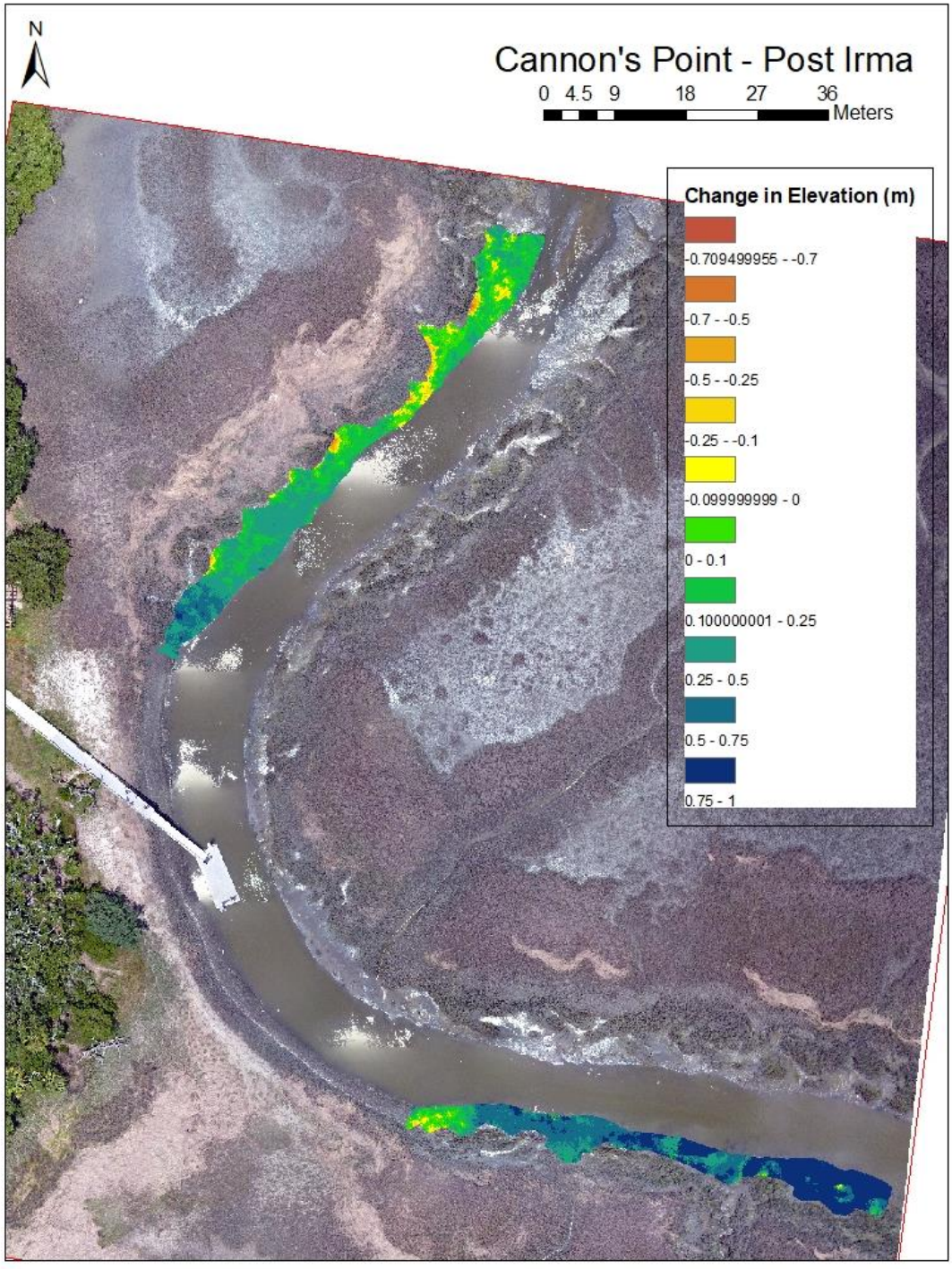


***Figure 16**: Changes in Cannon's Point streambank elevation post-Irma*

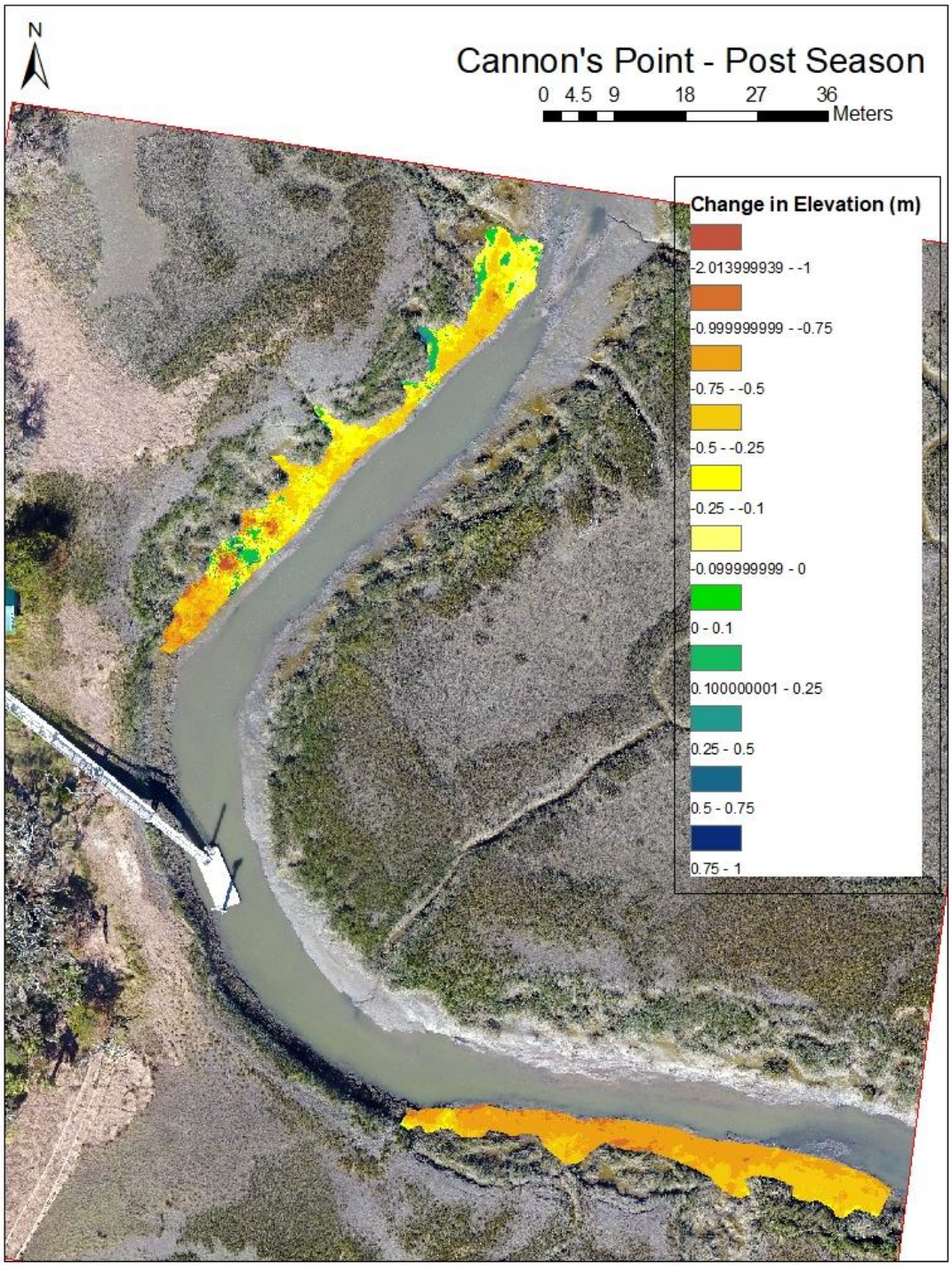


***Figure 17**: Changes in Cannon's Point streambank elevation post-season*

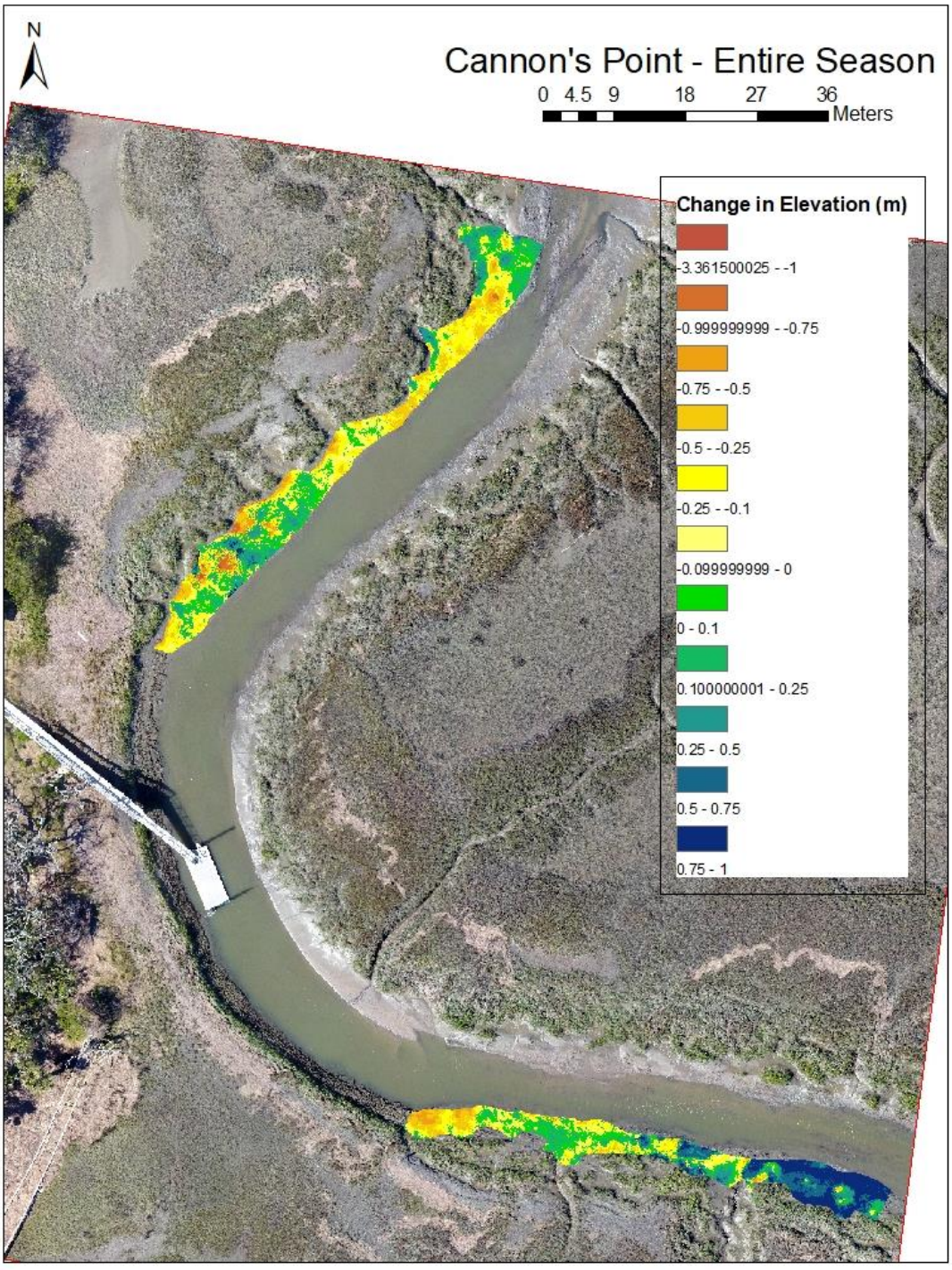


***Figure 18**: Cumulative changes in Cannon's Point streambank elevation*

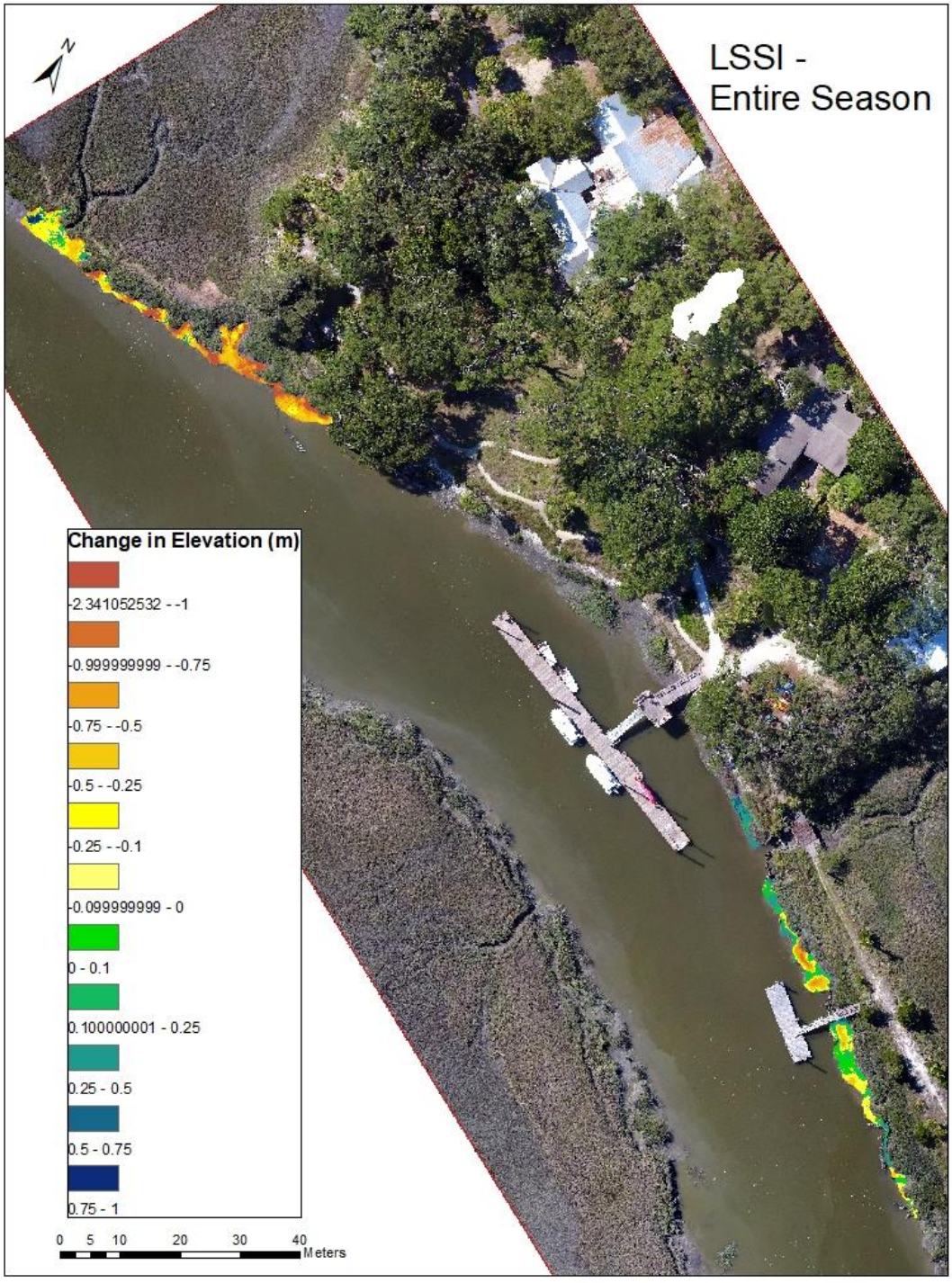


***Figure 19**: Cumulative changes to LSSI streambank elevation*

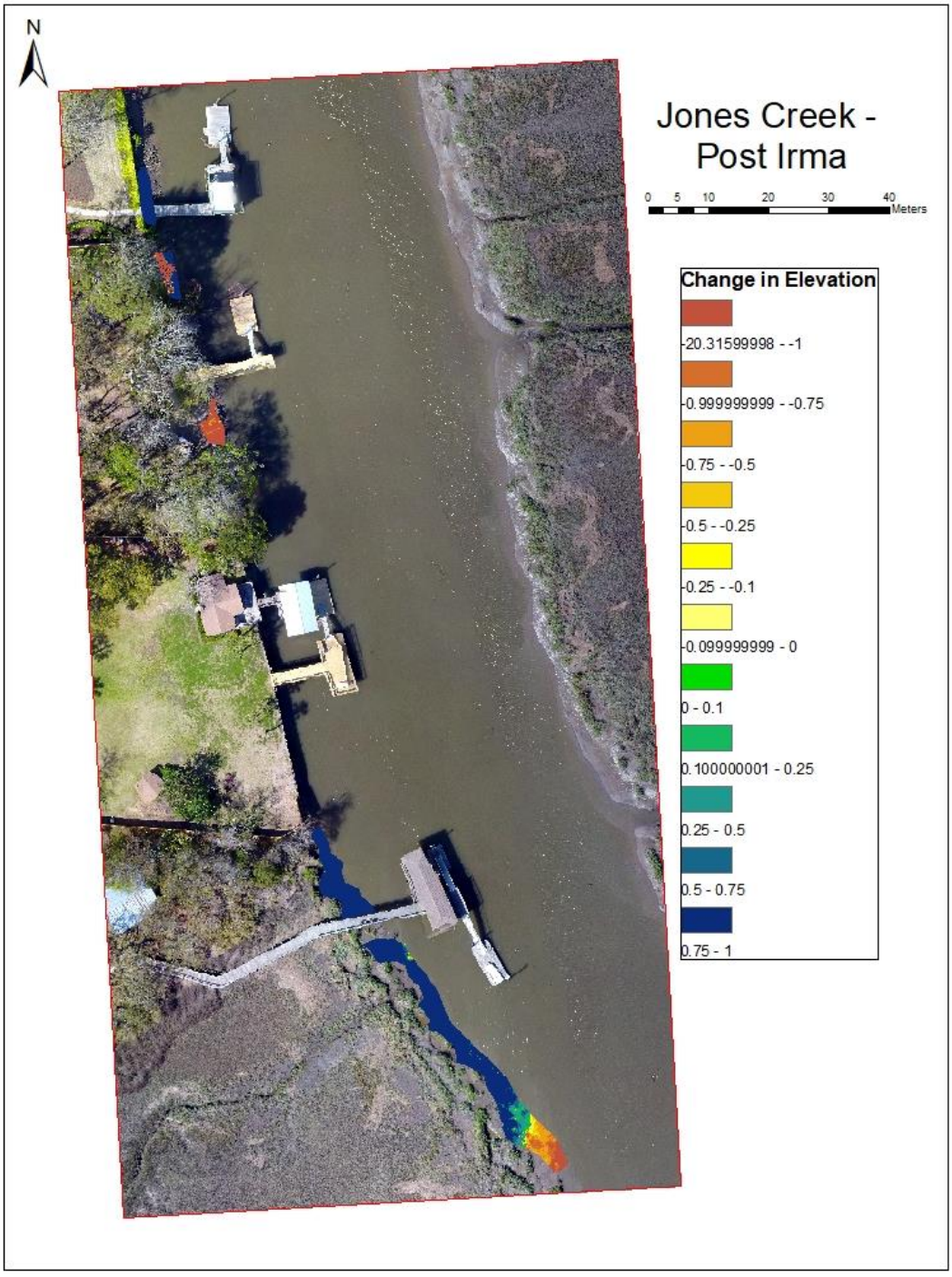


***Figure 20**: Changes in Jones Creek streambank elevation post-Irma*

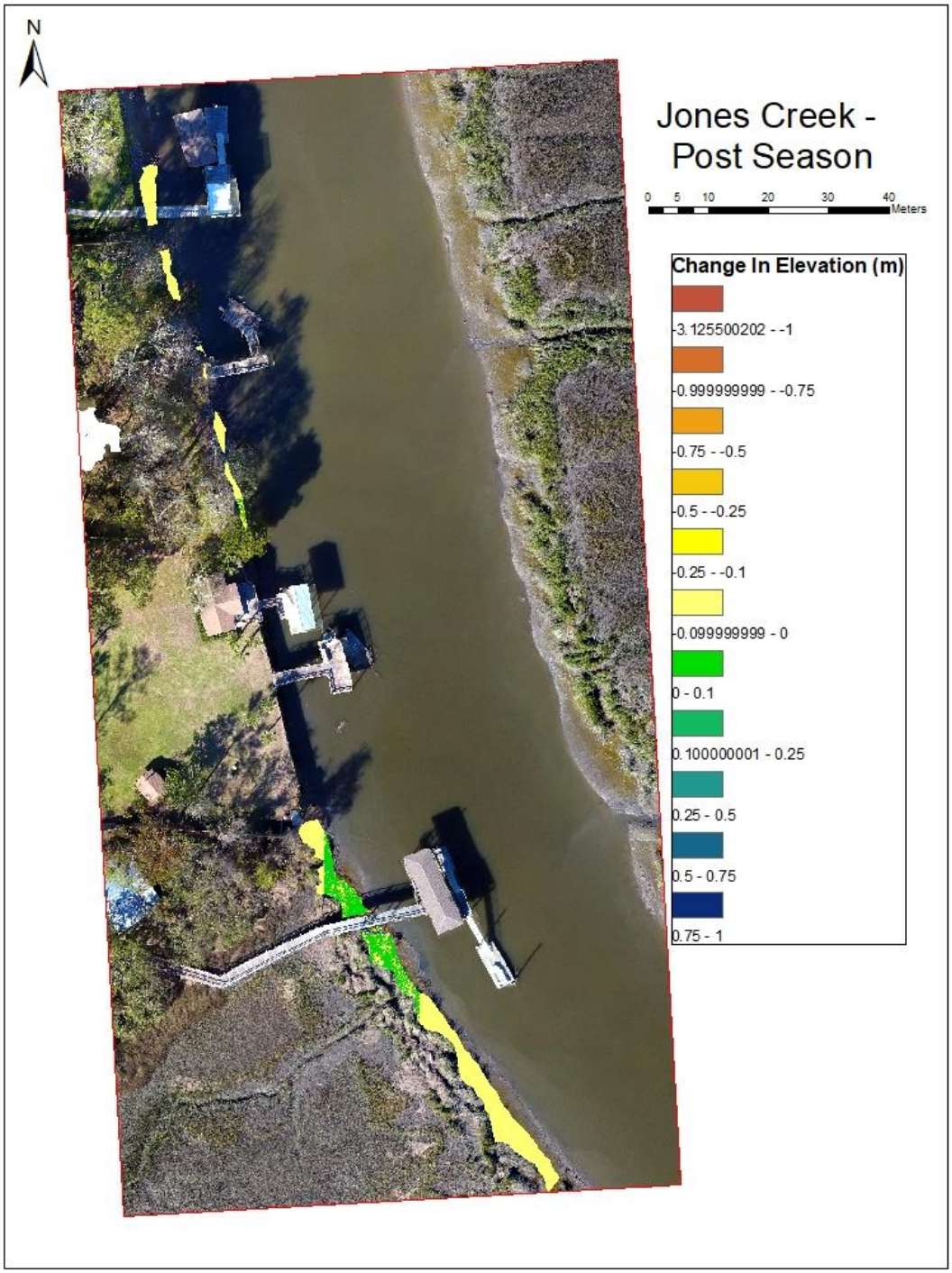


***Figure 21**: Changes in Jones Creek streambank elevation post-season*

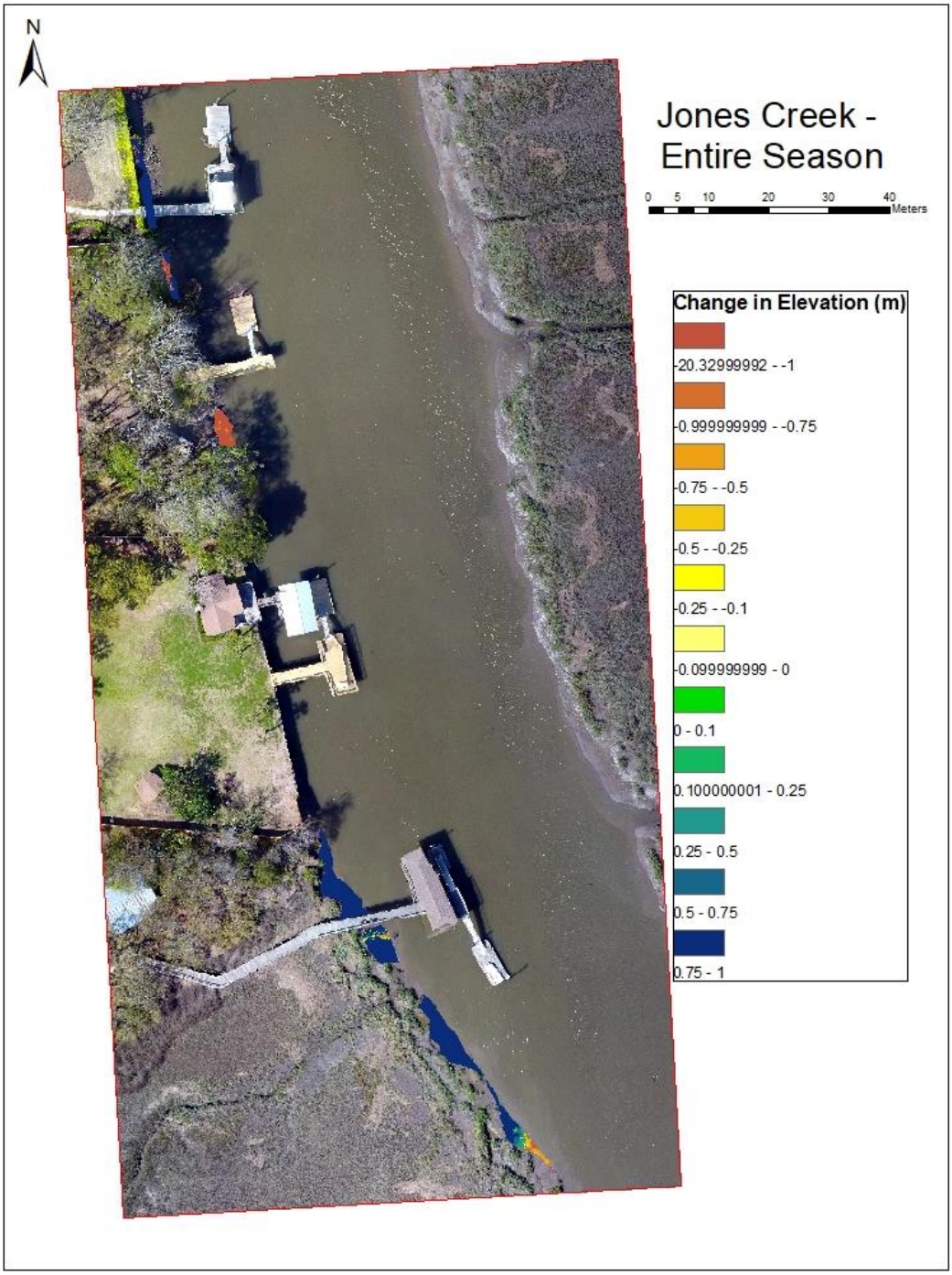


***Figure 22**: Cumulative changes to Jones Creek streambank elevation*

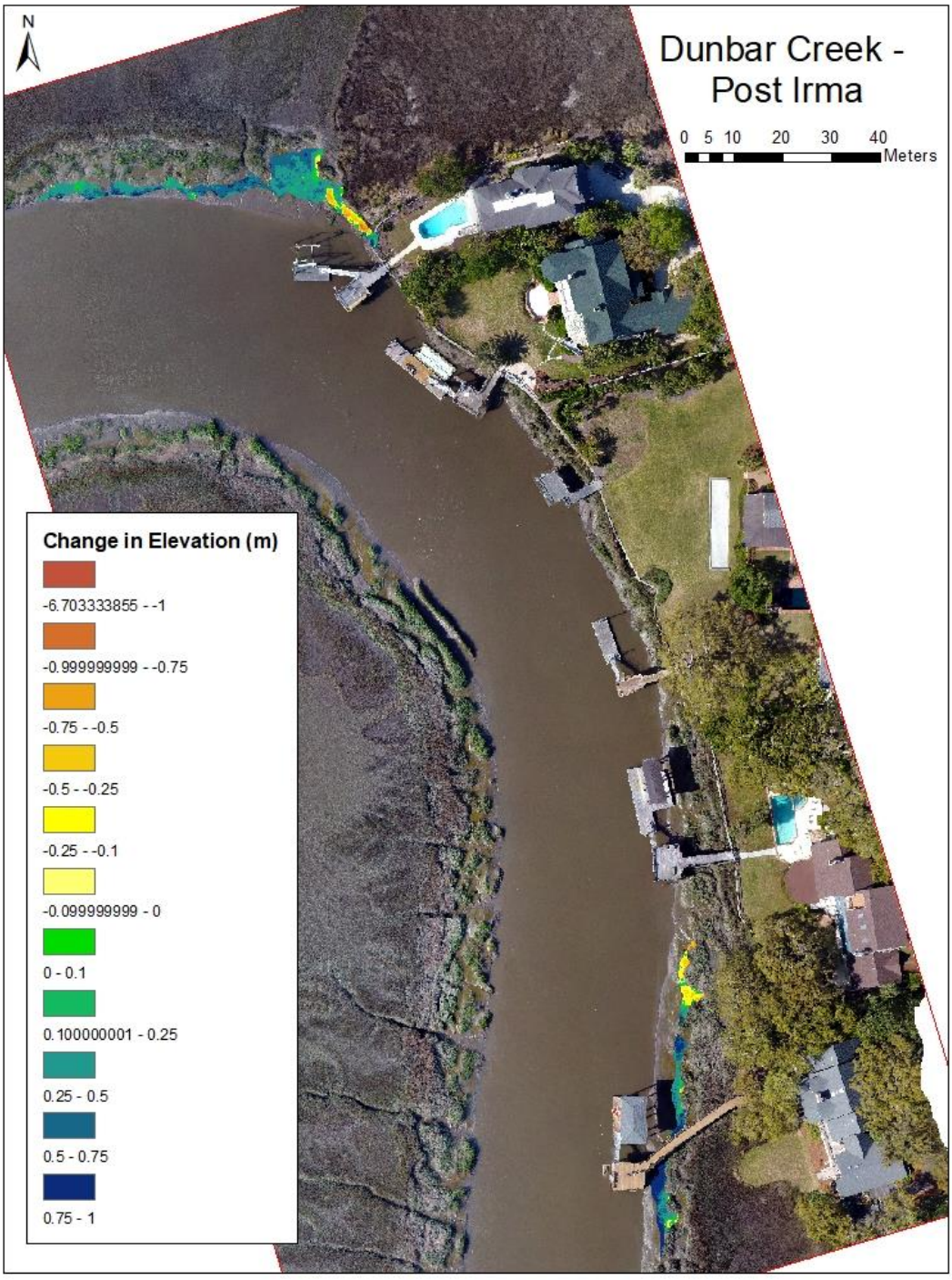


***Figure 23**: Changes to Dunbar Creek streambank elevation post-Irma*

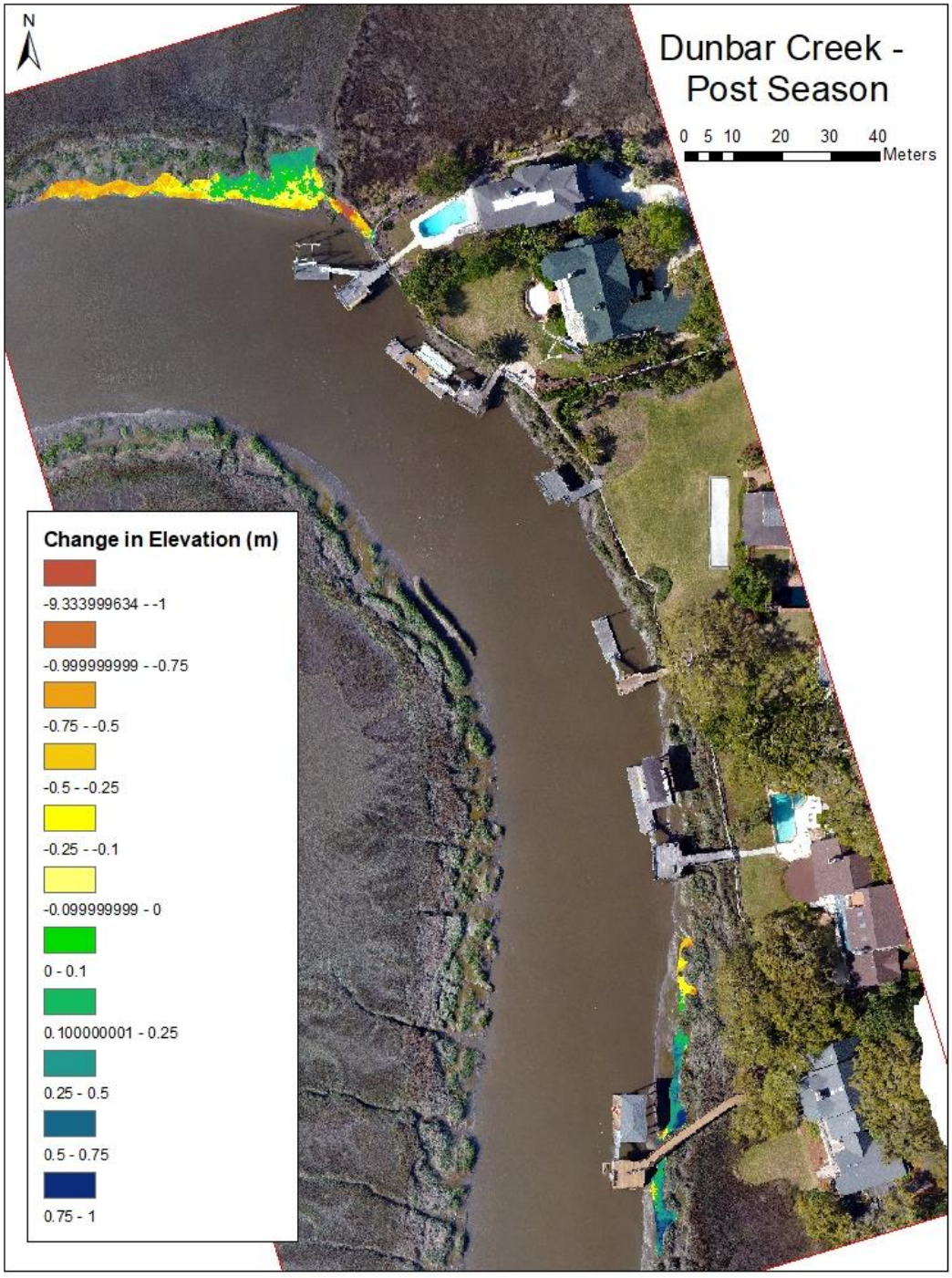


***Figure 24**: Changes in Dunbar Creek streambank elevation post-season*

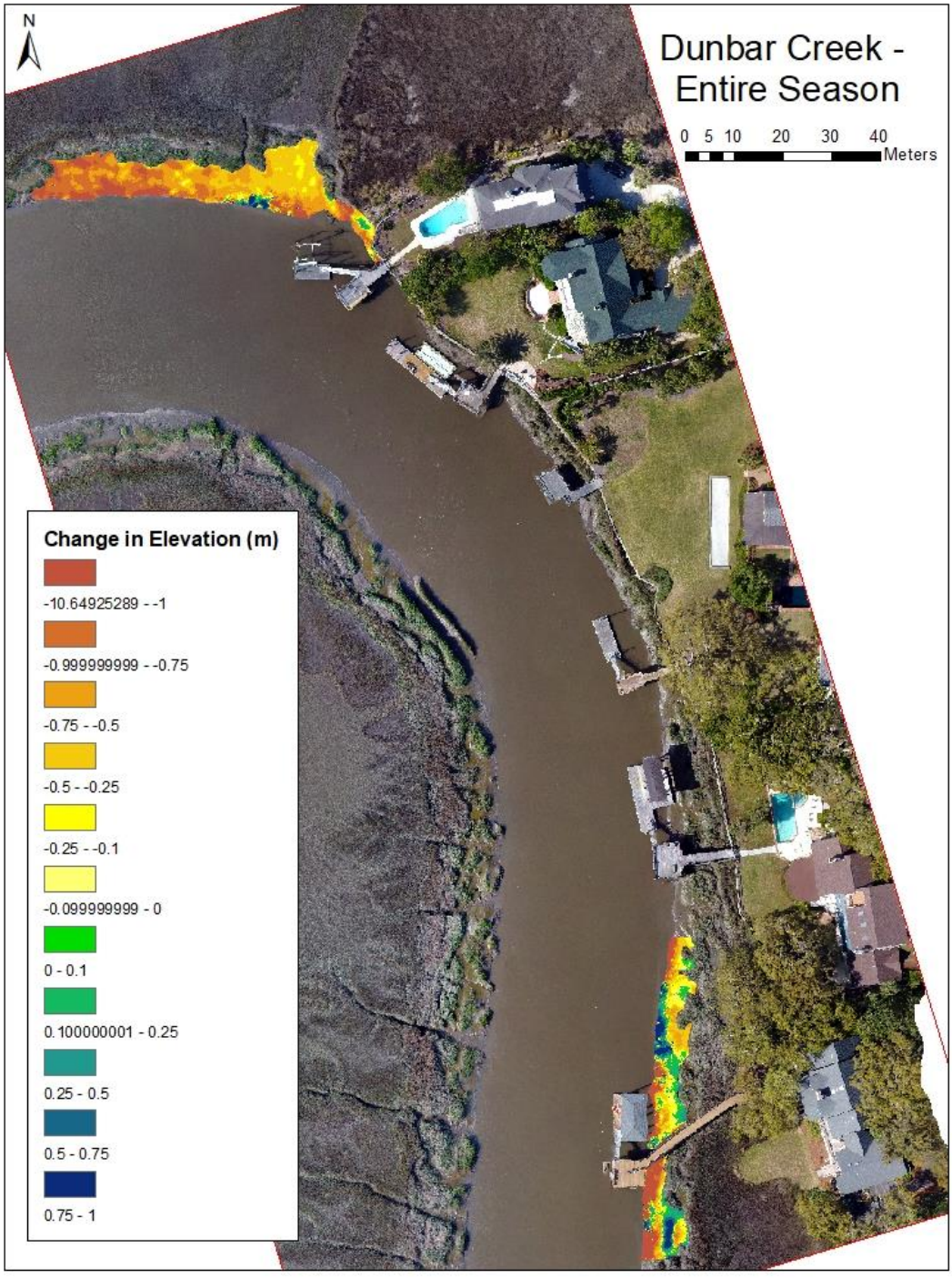


***Figure 25**: Cumulative changes in Dunbar Creek streambank elevation.*

### *Remotely Sensed Volumetric Changes*

Volumetric changes were calculated on a cubic meter per square meter basis, as the total area of each site differed. “Total Changes” refer to both upstream and downstream change, thus LSSI is omitted from this set. First glance indicates that bulkhead sites underwent much more accretion overall, but one must bear in mind that Jones Creek is included in this data and has likely skewed the results. Even so, the data is still highly variable (bulkheads more so than living shorelines) and shows no true significant difference (Figures 26-28). Erosion was observed at almost all downstream locations, which may indicate an increase in water velocity on the ebb tide and thus an increased erosive capacity on the downstream end of the structure. This could be taken into account when designing armoring structures in the future, with efforts to increase vegetation on the downstream side.

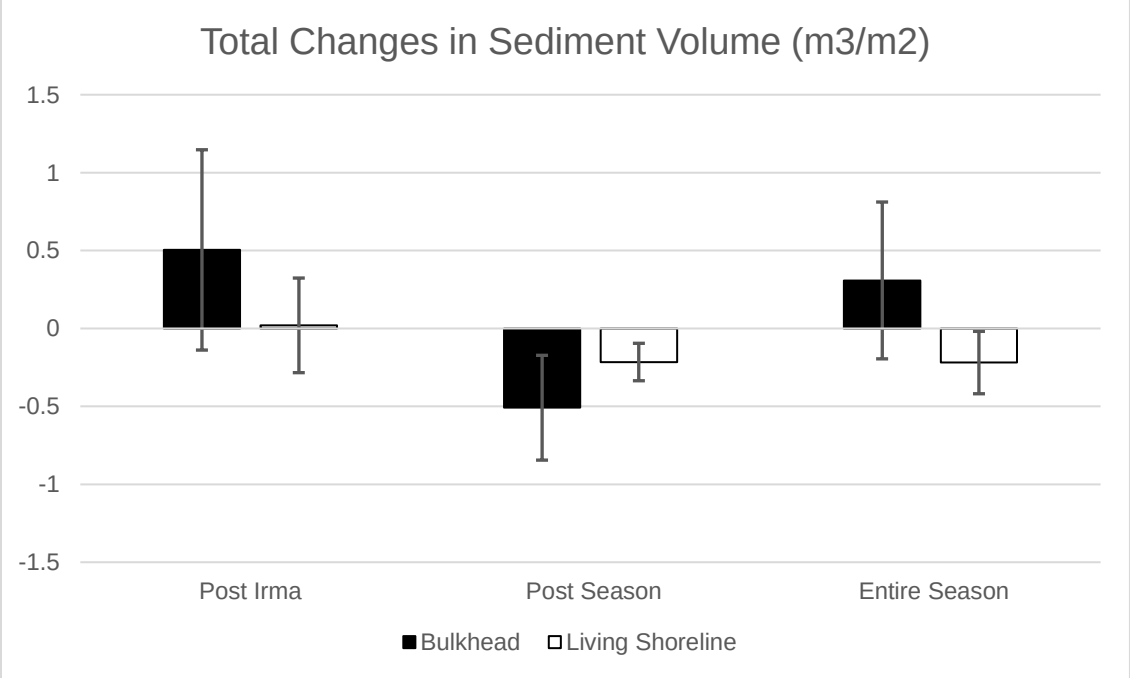


***Figure 26:*** *Changes in sediment volume both up and downstream from living shoreline and bulkhead sites presented with standard error. LSSI omitted.*

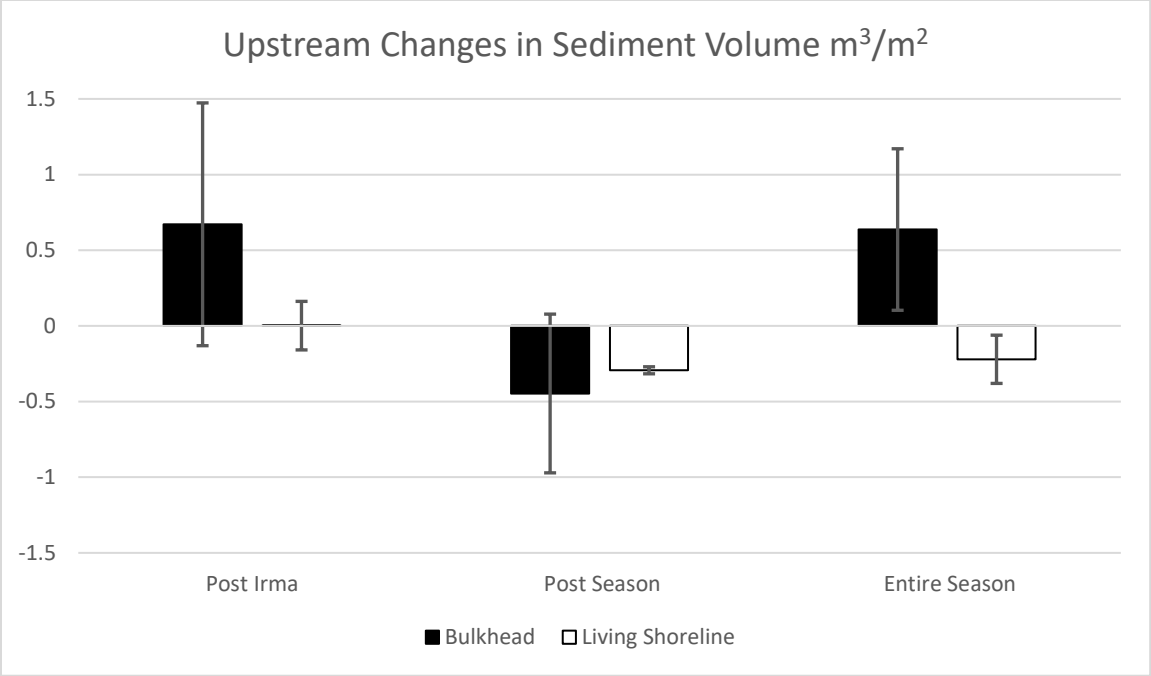


***Figure 27:*** *Changes in sediment volume upstream from living shoreline and bulkhead sites presented with standard error. LSSI included.*

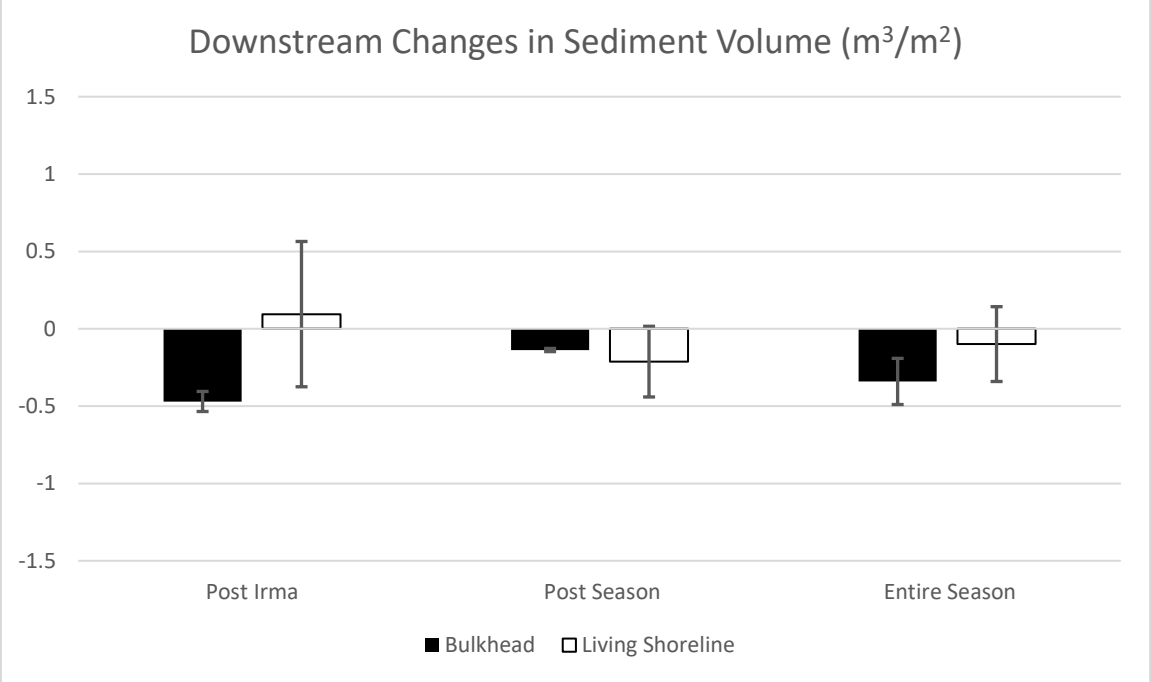


***Figure 28:*** *Changes in sediment volume downstream from living shoreline and bulkhead sites presented with standard error. LSSI included.*

***Remotely Sensed Erosion – Area of Influence***

An important question in analyzing the impact of hardened structures on our coastlines is, "How far does that impact extend?". In an effort to quantify this area of impact, two reference sites were chosen—the Dunbar Creek bulkhead and the Cannon's Point living shoreline—based on their similar vertical accuracy and seasonal behavior. The average change in elevation as one moves progressively further away from each structure are presented and discussed below (Figures 29-31). Each have been separated into upstream and downstream components so as to better observe variability in each channel.

Immediately following Irma, both sites showed overall increases in elevation, a proxy for accretion. However, we can see in Figure 29 that upstream, the bulkhead site is experiencing that accretion from 10-50 meters away from the structure (with erosion immediately adjacent), while the accretion at the living shoreline is more evenly distributed throughout. Downstream, the structures follow a similar pattern of accretion in the 10-50 m area, but the living shoreline generally accretes at a higher rate. Immediately adjacent to the structure however, the bulkhead erodes.

By the end of hurricane season, we observe downstream losses of sediment at both structures. The living shoreline is eroding at a steady pace throughout the 50-meter zone, while much more variability is observed at the bulkhead. Upstream, the bulkhead begins to accrete at 10 meters, but this change is again highly variable. The living shoreline maintains a steady pattern of erosion throughout the 50 meters.

Finally, we view the cumulative effects of hurricane season on these two structures, Downstream, we see the two truly diverge in the 35-50-meter zone, with accretion adjacent to the living shoreline and erosion adjacent to the bulkhead. Upstream, a similar pattern is followed but the bulkhead is markedly more erosive from 30-45 meters as well as more variable. It appears that the living shoreline, in addition to retaining more sediment throughout the season, also remains in a more constant state of equilibrium. It is still difficult to truly compare the two due their differences in age, length, and channel morphology. Particularly, the difference in age of the structures (some thirty years) makes direct comparison difficult. This does lead to surprising results, however. One would expect a channel to be in quite a state of flux after such a disturbance as armoring installation, which might indicate that Cannon's Point would be experiencing much more instability only two years post-armoring. This is not the case, however. Even thirty years post-installation, the bulkhead site is much more highly variable than the living shoreline site. Long term studies of Georgia's living shorelines will certainly prove interesting to test whether or not this channel stability relative to bulkhead sites holds true throughout the years.

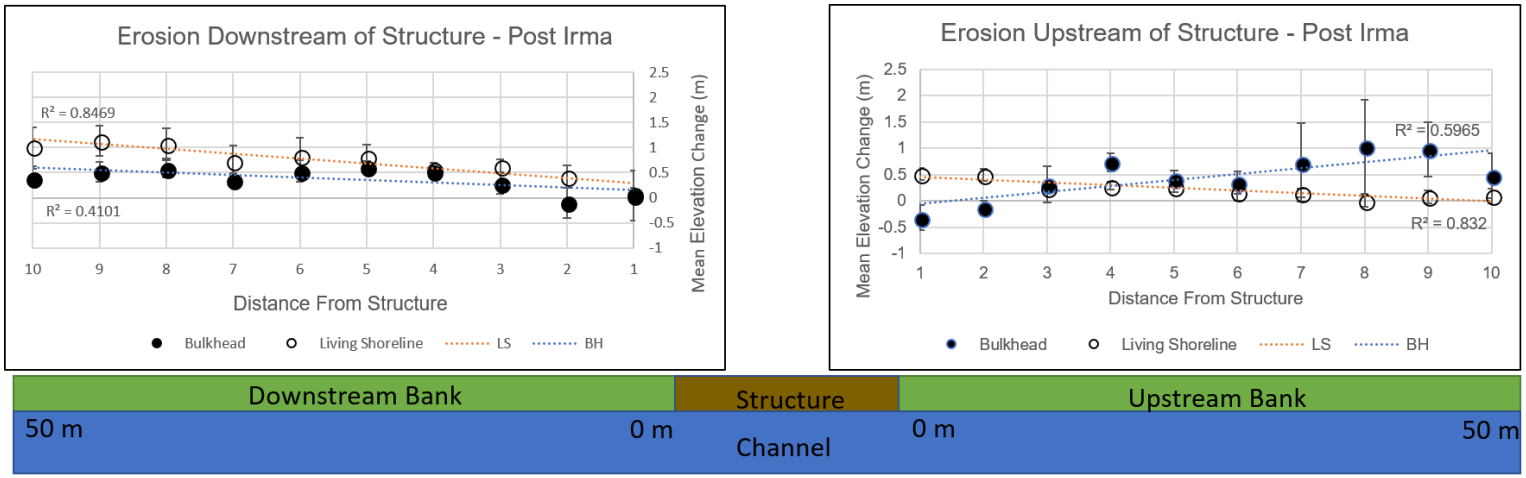


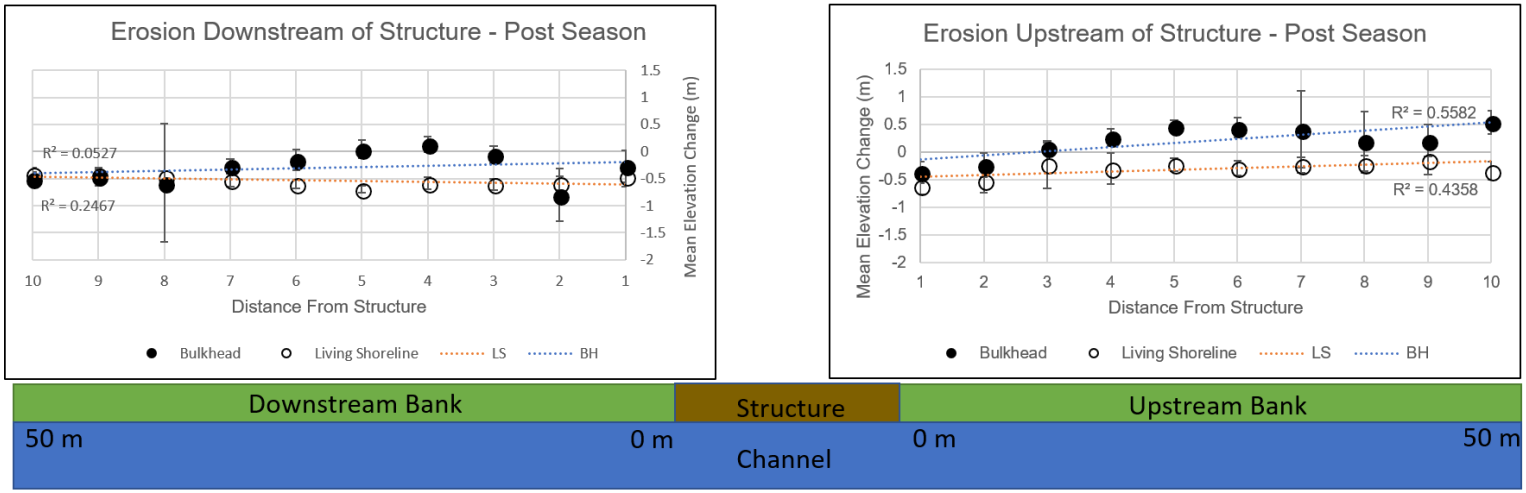


***Figure 29 (above)**: Erosion upstream and downstream of each armoring structure immediately following Hurricane Irma. Graphs are presented in such a way that data points represent their corresponding bank location if one were to view the site from a boat.*

***Figure 30 (below):** Erosion upstream and downstream of each structure at the end of hurricane season.*

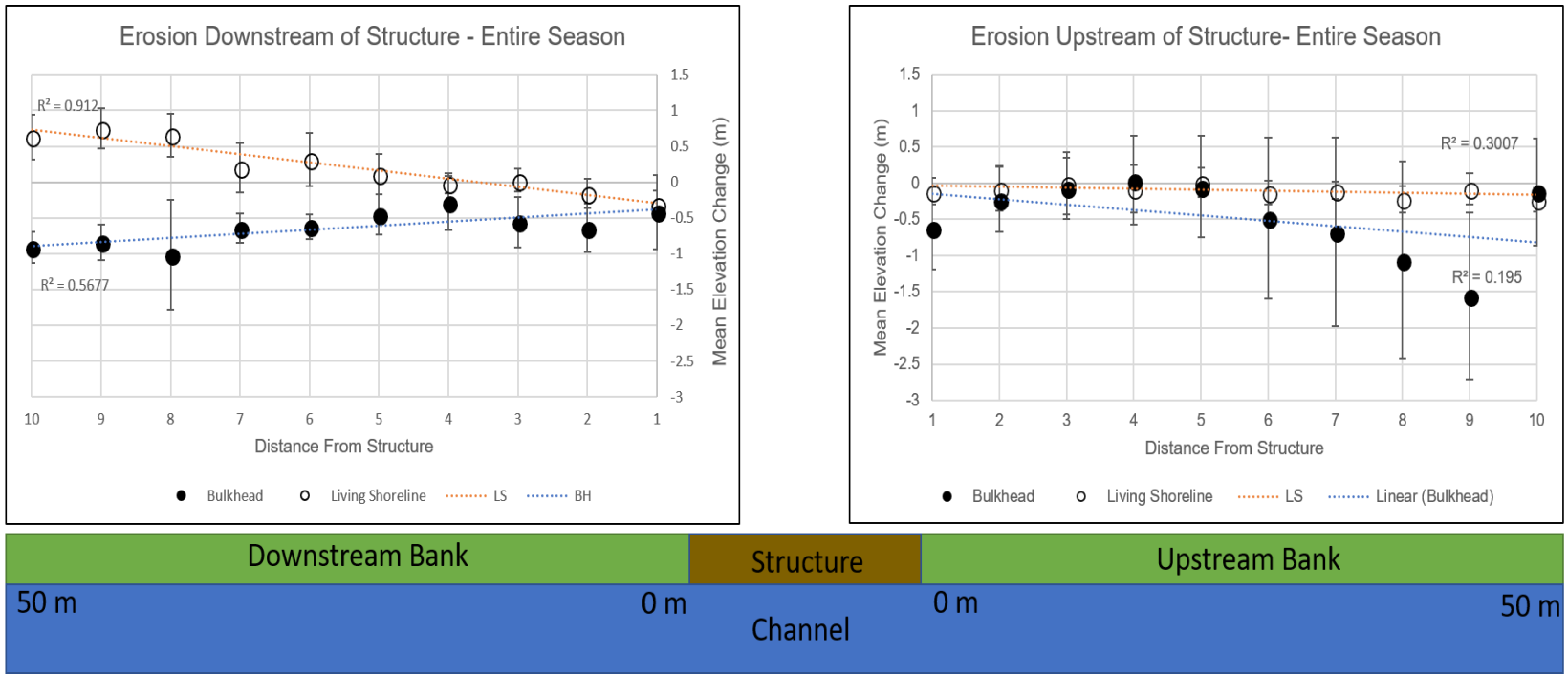


***Figure 31:*** *Cumulative erosion upstream and downstream from each structure throughout hurricane season. Graphs are presented in such a way that data points represent their corresponding bank locations if one were to view the site from a boat.*

# CHAPTER 4

# CONCLUSIONS

There are few, if any, concrete conclusions to be made from this initial dataset, but an endless number of possibilities for future research. The small sample size, variable environmental conditions, and hard lessons learned in the field may have provided few answers of statistical significance in the current study but leave us with an opportunity to build upon and refine the structure-from-motion method as a tool for coastal resource management. A number of improvements can be made to increase the accuracy of future data and work efficiency. First and foremost, future work would greatly benefit from a larger sample size. This will ultimately require an increase in the number of living shorelines available for study in Georgia, as well as opportunities to study living shorelines in higher energy environments. Without living shorelines in more variable environmental conditions, truly comparing them to their hard-armoring counterparts will remain impossible. Surveying larger expanses of bank, as well as including the opposite bank, would provide a more holistic view of the channels in question. As evidenced on Tybee Island, land use appears to have a strong influence on long term erosion trends and should be taken into account as well. Similarly, shoreline changes at Little St. Simons are likely influenced by boat traffic. Including this as a metric in future studies would further eliminate extraneous variability.

Finally, the timing of UAS flights should be much more tightly controlled in future studies. Varying water levels, lighting, and shadows led to losses of valuable data. Some of these issues could be addressed through careful site selection, but also through further data manipulation. Photo editing to brighten areas occluded by shadow should be experimented with, as should more advanced camera settings. Interdisciplinary research that includes the expertise of photographers as well as geographers and natural scientists could greatly improve the final product, as the SfM method is as much an art as it is a science. While data lost to high tides can only be corrected by better timing of flight, areas of bank occluded by marsh vegetation could be visualized if the height of marsh grass is carefully measured at the time of each flight. This could easily be performed using oblique imagery of each bank. For any future project, test flights and data processing—from start to finish—will be helpful in troubleshooting issues that are likely to arise in the field.

When using satellite imagery or aerial LiDAR to georeference, it is also of utmost importance that there be identifiable, unchanging features to use as ground control points. In especially undeveloped locations, or areas that have undergone significant construction, this method may not be possible, or may result in significant error. Access to quality georeferencing base data is also of concern. All communities are not so lucky as to have access to high resolution, open access base data. The affordability of and ease of access to these datasets on a global scale must be of top priority to all who conduct coastal research in the coming years, as vertical errors of even 0.5 meters increasingly become a matter of life or death.

Issues with the current study notwithstanding, the data gathered throughout the past year have provided a number of insights and questions for the future. The accuracies achieved here are well within a reasonable margin of error for many projects and can be improved upon by incorporating robust RTK-GPS ground control points. The issue of *access* however, both financially to equipment and physically to study sites remains a problem that can and should be addressed in future work. The erosion rates observed, though not significantly different between groups, do show patterns at specific locations. Scouring was observed adjacent to each bulkhead site, and areas adjacent to living shorelines appear to experience less variability on their adjacent banks. This dataset would most certainly benefit from additional years of observation, particularly in years without a major storm.

Though the SfM method is rife with challenges, it does show promise as a low-cost monitoring tool. The issues that arose in the current study can and should be addressed in the future, and improvements to this method should continue, particularly for use in vulnerable coastal areas.

Despite the lack of significant results presented currently, there are certain things that we already know. Living shorelines are a more ecologically sound choice than hard armoring. Their ecosystem services have been widely studied. An argument can be made that *all* armoring is simply a Band-Aid in the face of rising seas, but living shorelines have proven themselves to be a *better* Band-Aid. It is not unreasonable to choose the stop-gap that comes with habitat, water filtration, and self-healing. It is not unreasonable to provide ecosystem services to a coastline in peril when that alternative exists. One could even go as far as to say it's a good idea.

## LITERATRE CITED


Balouskus, R. G., & Targett, T. E. (2016). Fish and Blue Crab Density along a Riprap-Sill-Hardened Shoreline: Comparisons with Spartina Marsh and Riprap. *Transactions of the American Fisheries Society, 145*(4), 766-773. doi:10.1080/00028487.2016.1172508

Beck, M. W., Brumbaugh, R. D., Airoldi, L., Carranza, A., Coen, L. D., Crawford, C., . . . Guo, X. M. (2011). Oyster Reefs at Risk and Recommendations for Conservation, Restoration, and Management. *Bioscience, 61*(2), 107-116. doi:10.1525/bio.2011.61.2.5

Bilkovic, D. M., Mitchell, M., Mason, P., & Duhring, K. (2016). The Role of Living Shorelines as Estuarine Habitat Conservation Strategies. *Coastal Management, 44*(3), 161-174. doi:10.1080/08920753.2016.1160201

Bilkovic, D. M., & Mitchell, M. M. (2013). Ecological tradeoffs of stabilized salt marshes as a shoreline protection strategy: Effects of artificial structures on macrobenthic assemblages. *Ecological Engineering, 61*, 469-481. doi:10.1016/j.ecoleng.2013.10.011

Bilkovic, D. M., & Roggero, M. M. (2008). Effects of coastal development on nearshore estuarine nekton communities. *Marine Ecology Progress Series, 358*, 27-39. doi:10.3354/meps07279

Blender Foundation, S. (2017). Blender 2.79. Amstredam, the Netherlands: Stichting Blender Foundation.

Brandon, C. M., Woodruff, J. D., Orton, P. M., & Donnelly, J. P. (2016). Evidence for elevated coastal vulnerability following large-scale historical oyster bed harvesting. *Earth Surface Processes and Landforms, 41*(8), 1136-1143. doi:10.1002/esp.3931

Brunier, G., Fleury, J., Anthony, E. J., Gardel, A., & Dussouillez, P. (2016). Close-range airborne Structure-from-Motion Photogrammetry for high-resolution beach morphometric surveys: Examples from an embayed rotating beach. *Geomorphology, 261*, 76-88. doi:10.1016/j.geomorph.2016.02.025

Brunier, G., Fleury, J., Anthony, E. J., Pothin, V., Vella, C., Dussouillez, P., . . . Michaud, E. (2016). Structure-from-Motion photogrammetry for high-resolution coastal and fluvial geomorphic surveys. *Geomorphologie-Relief Processus Environnement, 22*(2), 147-161. doi:10.4000/geomorphologie.11358

Casella, E., Rovere, A., Pedroncini, A., Stark, C. P., Casella, M., Ferrari, M., & Firpo, M. (2016). Drones as tools for monitoring beach topography changes in the Ligurian Sea (NW Mediterranean). *Geo-Marine Letters, 36*(2), 151-163. doi:10.1007/s00367-016-0435-9

Christian, P., & Davis, J. (2016). Hillslope gully photogeomorphology using structure-from-motion. *Zeitschrift Fur Geomorphologie, 60*, 59-78. doi:10.1127/zfg_suppl/2016/00238

Colden, A. M., Fall, K. A., Cartwright, G. M., & Friedrichs, C. T. (2016). Sediment Suspension and Deposition Across Restored Oyster Reefs of Varying Orientation to Flow: Implications for Restoration. *Estuaries and Coasts, 39*(5), 1435-1448. doi:10.1007/s12237-016-0096-y

Cook, K. L. (2017). An evaluation of the effectiveness of low-cost UAVs and structure from motion for geomorphic change detection. *Geomorphology, 278*, 195-208. doi:10.1016/j.geomorph.2016.11.009

Couranz, K. (2018). Oysters. *Fish Facts.* Retrieved from https://chesapeakebay.noaa.gov/index.php?option=com_content&view=article&id=201&Itemid=200

De Roo, S., & Troch, P. (2015). Evaluation of the Effectiveness of a Living Shoreline in a Confined, Non-Tidal Waterway Subject to Heavy Shipping Traffic. *River Research and Applications, 31*(8), 1028-1039. doi:10.1002/rra.2790

Dietrich, J. T. (2017). Bathymetric Structure-from-Motion: extracting shallow stream bathymetry from multi-view stereo photogrammetry. *Earth Surface Processes and Landforms, 42*(2), 355-364. doi:10.1002/esp.4060

Gittman, R. K., Fodrie, F. J., Popowich, A. M., Keller, D. A., Bruno, J. F., Currin, C. A., . . . Piehler, M. F. (2015). Engineering away our natural defenses: an analysis of shoreline hardening in the US. *Frontiers in Ecology and the Environment, 13*(6), 301-307. doi:10.1890/150065

Gittman, R. K., Peterson, C. H., Currin, C. A., Fodrie, F. J., Piehler, M. F., & Bruno, J. F. (2016). Living shorelines can enhance the nursery role of threatened estuarine habitats. *Ecological Applications, 26*(1), 249-263. doi:10.1890/14-0716

Gittman, R. K., Popowich, A. M., Bruno, J. F., & Peterson, C. H. (2014). Marshes with and without sills protect estuarine shorelines from erosion better than bulkheads during a Category 1 hurricane. *Ocean & Coastal Management, 102*, 94-102. doi:10.1016/j.ocecoaman.2014.09.016

Gittman, R. K., Scyphers, S. B., Smith, C. S., Neylan, I. P., & Grabowski, J. H. (2016). Ecological Consequences of Shoreline Hardening: A Meta-Analysis. *Bioscience, 66*(9), 763-773. doi:10.1093/biosci/biw091

Hayes, D. A., Timmer, E. R., Deutsch, J. L., Ranger, M. J., & Gingras, M. K. (2017). Analyzing Dune Foreset Cyclicity In Outcrop With Photogrammetry. *Journal of Sedimentary Research, 87*(1), 66-74. doi:10.2110/jsr.2016.93

Humphries, A. T., & La Peyre, M. K. (2015). Oyster reef restoration supports increased nekton biomass and potential commercial fishery value. *Peerj, 3*, 19. doi:10.7717/peerj.1111

Jackson, C. W., Alexander, C. R., & Bush, D. M. (2012). Application of the AMBUR R package for spatio-temporal analysis of shoreline change: Jekyll Island, Georgia, USA. *Computers & Geosciences, 41*, 199-207. doi:10.1016/j.cageo.2011.08.009

Jaud, M., Grasso, F., Le Dantec, N., Verney, R., Delacourt, C., Ammann, J., . . . Grandjean, P. (2016). Potential of UAVs for Monitoring Mudflat Morphodynamics (Application to the Seine Estuary, France). *Isprs International Journal of Geo-Information, 5*(4), 20. doi:10.3390/ijgi5040050

Javernick, L., Hicks, D., Measures, R., Caruso, B., & Brasington, J. (2015). Numerical Modelling of Braided Rivers with Structure-from-Motion-Derived Terrain Models. *River Research and Applications*.

Kennish, M. J. (2001). Coastal salt marsh systems in the US: A review of anthropogenic impacts. *Journal of Coastal Research, 17*(3), 731-748.

Klemas, V. V. (2015). Coastal and Environmental Remote Sensing from Unmanned Aerial Vehicles: An Overview. *Journal of Coastal Research, 31*(5), 1260-1267. doi:10.2112/jcoastres-d-15-00005.1

Leonard, L. A., Wren, P. A., & Beavers, R. L. (2002). Flow dynamics and sedimentation in Spartina alterniflora and Phragmites australis marshes of the Chesapeake Bay. *Wetlands, 22*(2), 415-424. doi:10.1672/0277-5212(2002)022[0415:fdasis]2.0.co;2

Long, N., Millescamps, B., Guillot, B., Pouget, F., & Bertin, X. (2016). Monitoring the Topography of a Dynamic Tidal Inlet Using UAV Imagery. *Remote Sensing, 8*(5), 18. doi:10.3390/rs8050387

Long, N., Millescamps, B., Pouget, F., Dumon, A., Lachaussee, N., & Bertin, X. (2016). ACCURACY ASSESSMENT OF COASTAL TOPOGRAPHY DERIVED FROM UAV IMAGES. *XXIII ISPRS Congress, Commission I, 41*(B1), 1127-1134. doi:10.5194/isprsarchives-XLI-B1-1127-2016

Long, N., Millescamps, B., Pouget, F., Dumon, A., Lachaussee, N., & Bertin, X. (2016 b). Accuracy Assessment of Coastal Topography Derived from UAV Images. *XXIII ISPRS Congress, Commission I, 41*(B1), 1127-1134. doi:10.5194/isprsarchives-XLI-B1-1127-2016

Lu, C. H. (2016). Applying UAV and photogrammetry to monitor the morphological changes along the beach in Penghu islands. *Xxiii Isprs Congress, Commission Viii, 41*(B8), 1153-1156. doi:10.5194/isprsarchives-XLI-B8-1153-2016

MA, (Millenium Ecosystem Assessment), . (2005). *Ecosystems and human well-being*. Washington D.C.: Island Press

Mancini, F., Dubbini, M., Gattelli, M., Stecchi, F., Fabbri, S., & Gabbianelli, G. (2013). Using Unmanned Aerial Vehicles (UAV) for High-Resolution Reconstruction of Topography: The Structure from Motion Approach on Coastal Environments. *Remote Sensing, 5*(12), 6880-6898. doi:10.3390/rs5126880

Manis, J. E., Garvis, S. K., Jachec, S. M., & Walters, L. J. (2015). Wave attenuation experiments over living shorelines over time: a wave tank study to assess recreational boating pressures. *Journal of Coastal Conservation, 19*(1), 1-11. doi:10.1007/s11852-014-0349-5

MAREX, U. (2018). Oyster Reefs in Georgia. Retrieved from http://gacoast.uga.edu/outreach/programs/oyster-reefs-georgia/

Marteau, B., Vericat, D., Gibbins, C., Batalla, R. J., & Green, D. R. (2017). Application of Structure-from-Motion photogrammetry to river restoration. *Earth Surface Processes and Landforms, 42*(3), 503-515. doi:10.1002/esp.4086

Nordstrom, K. F., Jackson, N. L., Rafferty, P., Raineault, N. A., & Grafals-Soto, R. (2009). Effects of Bulkheads on Estuarine Shores: an Example from Fire Island National Seashore, USA. *Journal of Coastal Research*, 188-192.

Nouwakpo, S. K., Weltz, M. A., & McGwire, K. (2016). Assessing the performance of structure-from-motion photogrammetry and terrestrial LiDAR for reconstructing soil surface microtopography of naturally vegetated plots. *Earth Surface Processes and Landforms, 41*(3), 308-322. doi:10.1002/esp.3787

Nouwakpo, S. K., Weltz, M. A., McGwire, K. C., Williams, J. C., Osama, A. H., & Green, C. H. M. (2017). Insight into sediment transport processes on saline rangeland hillslopes using three-dimensional soil microtopography changes. *Earth Surface Processes and Landforms, 42*(4), 681-696. doi:10.1002/esp.4013

NRC, (National Research Council),. (2007). *Mitigating shore erosion along sheltered coasts.* Washington D.C.: National Academies Press.

O'Donnell, J. E. D. (2017). Living Shorelines: A Review of Literature Relevant to New England Coasts. *Journal of Coastal Research, 33*(2), 435-451. doi:10.2112/jcoastres-d-15-00184.1

Papakonstantinou, A., Topouzelis, K., & Pavlogeorgatos, G. (2016). Coastline Zones Identification and 3D Coastal Mapping Using UAV Spatial Data. *Isprs International Journal of Geo-Information, 5*(6), 14. doi:10.3390/ijgi5060075

Peters, J. R., Yeager, L. A., & Layman, C. A. (2015). Comparison of fish assemblages in restored and natural mangrove habitats along an urban shoreline. *Bulletin of Marine Science, 91*(2), 125-139. doi:10.5343/bms.2014.1063

Prosdocimi, M., Calligaro, S., Sofia, G., Dalla Fontana, G., & Tarolli, P. (2015). Bank erosion in agricultural drainage networks: new challenges from structure-from-motion photogrammetry for post-event analysis. *Earth Surface Processes and Landforms, 40*(14), 1891-1906. doi:10.1002/esp.3767

Redfield, A. C. (1972). Development of a New England Salt Marsh. *Ecological Monographs, 42*(2), 201-237. doi:10.2307/1942263

Rodriguez, A. B., Fodrie, F. J., Ridge, J. T., Lindquist, N. L., Theuerkauf, E. J., Coleman, S. E., . . . Kenworthy, M. D. (2014). Oyster reefs can outpace sea-level rise. *Nature Climate Change, 4*(6), 493-497. doi:10.1038/nclimate2216

Scyphers, S. B., Picou, J. S., & Powers, S. P. (2015). Participatory Conservation of Coastal Habitats: The Importance of Understanding Homeowner Decision Making to Mitigate Cascading Shoreline Degradation. *Conservation Letters, 8*(1), 41-49. doi:10.1111/conl.12114

Scyphers, S. B., Powers, S. P., & Heck, K. L. (2015). Ecological Value of Submerged Breakwaters for Habitat Enhancement on a Residential Scale. *Environmental Management, 55*(2), 383-391. doi:10.1007/s00267-014-0394-8

Scyphers, S. B., Powers, S. P., Heck, K. L., & Byron, D. (2011). Oyster Reefs as Natural Breakwaters Mitigate Shoreline Loss and Facilitate Fisheries. *Plos One, 6*(8), 12. doi:10.1371/journal.pone.0022396

Sharma, S., Goff, J., Cebrian, J., & Ferraro, C. (2016). A hybrid shoreline stabilization technique: Impact of modified intertidal reefs on marsh expansion and nekton habitat in the northern Gulf of Mexico. *Ecological Engineering, 90*, 352-360. doi:10.1016/j.ecoleng.2016.02.003

Smith, C. S., Gittman, R. K., Neylan, I. P., Scyphers, S. B., Morton, J. P., Fodrie, F. J., . . . Peterson, C. H. (2017). Hurricane damage along natural and hardened estuarine shorelines: Using homeowner experiences to promote nature-based coastal protection. *Marine Policy, 81*, 350-358. doi:10.1016/j.marpol.2017.04.013

Theuerkauf, S. J., Eggleston, D. B., Puckett, B. J., & Theuerkauf, K. W. (2017). Wave Exposure Structures Oyster Distribution on Natural Intertidal Reefs, But Not on Hardened Shorelines. *Estuaries and Coasts, 40*(2), 376-386. doi:10.1007/s12237-016-0153-6

Toft, J. D., Ogston, A. S., Heerhartz, S. M., Cordell, J. R., & Flemer, E. E. (2013). Ecological response and physical stability of habitat enhancements along an urban armored shoreline. *Ecological Engineering, 57*, 97-108. doi:10.1016/j.ecoleng.2013.04.022

Turner, I. L., Harley, M. D., & Drummond, C. D. (2016). UAVs for coastal surveying. *Coastal Engineering, 114,* 19-24. doi:10.1016/j.coastaleng.2016.03.011

USGS. (2017). *Agisoft PhotoScan Workflow*.

Ventura, D., Bruno, M., Lasinio, G. J., Belluscio, A., & Ardizzone, G. (2016). A low-cost drone based application for identifying and mapping of coastal fish nursery grounds. *Estuarine Coastal and Shelf Science, 171,* 85-98. doi:10.1016/j.ecss.2016.01.030

Wakefield, K. (2016). Assessing Shoreline Change and Vegetation Cover Adjacent to Back-Barrier Shoreline Stabilization Structures in Georgia Estuaries (1).pdf>.

Wang, A., Wang, Y., & Chen, J. (2008). Role of Spartina alterniflora on sediment dynamics of coastal salt marshes — case study from central Jiangsu and middle Fujian coasts. *Frontiers of Earth Science in China, 2*(3), 269-275. doi:10.1007/s11707-008-0021-1

Yoo, C. I., & Oh, T. S. (2016). Beach Volume Change Using UAV Photogrammetry Songjung Beach, Korea. *Xxiii Isprs Congress, Commission Viii, 41*(B8), 1201-1205. doi:10.5194/isprsarchives-XLI-B8-1201-2016

## APPENDIX I

## TYBEE ISLAND HISTORIC ORTHOPHOTOS

**1951**

**1971**

**1994**

**2009**

**2015**